35e jaargang 2013 nummer 2 issn 1381 - 4842

TIJDSCHRIFT VOOR NUCLEAIRE GENEESKUNDE

Regadenoson

^{18}F-FDG dosering

Een gastrocolocutane fistel

Rapiscan®
regadenoson

IDB Holland bv
From Atom to Image

Now this won't take a minute...

Rapiscan is the only standard dose, infusion pump-free, selective coronary vasodilator for use as a pharmacological stress agent for radionuclide myocardial perfusion imaging.

- Administer Rapiscan as a full 10 sec IV injection
- Flush immediately with 5ml saline
- Deliver radiotracer 10-20 seconds after saline flush

Stress simplified by design

RAPISCAN® ▼ (regadenoson)
ABBREVIATED PRESCRIBING INFORMATION

PRESCRIBERS SHOULD READ THE SUMMARY OF PRODUCT CHARACTERISTICS (SPC) Rapiscan vials contain regadenoson (400 microgram solution for injection). Indication: Pharmacological stress agent for radionuclide myocardial perfusion imaging in adult patients which are unable to undergo adequate exercise stress. Dosage and Administration: Each 5 mL vial contains 400 micrograms regadenoson, which is injected over 10 seconds into a peripheral vein followed by 5 mL saline (0.9% sodium chloride) solution flush. The radiopharmaceutical should be administered 10-20 seconds after saline injection. The same catheter may be used for Rapiscan and the radiopharmaceutical. Patients should avoid consumption of any products containing methylxanthines (e.g. caffeine) as well as any medicinal products containing theophylline for at least 12 hours before Rapiscan administration. When possible, dipyridamole should be withheld for at least two days prior to Rapiscan administration. Contra-indications: Hypersensitivity to active substance or excipients; patients with second or third degree AV block or sinus node dysfunction who do not have a functioning artificial pacemaker; unstable angina that has not been stabilised with medical therapy; severe hypotension; decompensated heart failure. Precautions: Rapiscan has the potential to cause serious and life-threatening reactions. Continuous ECG monitoring should be performed and vital signs monitored at frequent intervals until ECG parameters, heart rate and blood pressure have returned to pre-dose levels. Aminophylline may be administered by slow intravenous injection to attenuate severe and/or persistent adverse reactions to Rapiscan. Fatal cardiac arrest, life-threatening ventricular arrhythmias, and myocardial infarction may result from the ischaemia induced by pharmacologic stress agents like regadenoson. Adenosine receptor agonists including regadenoson can depress the sinoatrial (SA) and AV nodes and may cause first, second or third degree AV block, or sinus bradycardia. Adenosine receptor agonists including regadenoson induce arterial vasodilation and hypotension. The risk of serious hypotension may be higher in patients with autonomic dysfunction, hypovolemia, left main coronary artery stenosis, stenotic valvular heart disease, pericarditis or pericardial effusions, or stenotic carotid artery disease with cerebrovascular insufficiency. Adenosine receptor agonists may cause bronchoconstriction and respiratory compromise. For patients with known or suspected bronchoconstrictive disease, chronic obstructive pulmonary disease (COPD) or asthma, appropriate bronchodilator therapy and resuscitative measures should be available prior to Rapiscan administration. Regadenoson stimulates sympathetic output and may increase the risk of ventricular tachyarrhythmias in patients with a long QT syndrome. This medicinal product contains less than 1 mmol sodium (23 mg) per dose. However, the injection of sodium chloride 9 mg/ml (0.9%) solution given after Rapiscan contains 45 mg of sodium. To be taken into consideration by patients on a controlled sodium diet. Undesirable effects: Adverse reactions in most patients were mild, transient (usually resolving within 30 minutes) and required no medical intervention. Rapiscan may cause myocardial ischaemia, hypotension leading to syncope and transient ischaemic attacks, and SA/AV node block requiring intervention. Aminophylline may be used to attenuate severe or persistent adverse reactions. Very common adverse events reported were dyspnoea, headache, flushing, chest pain, electrocardiogram ST changes, gastrointestinal discomfort, and dizziness. Common adverse events reported were paraesthesia, hypoaesthesia, dysgeusia, angina pectoris, atrioventricular block, tachycardia, palpitations, other ECG abnormalities including electrocardiogram QT corrected interval prolonged, hypotension, throat tightness, throat irritation, cough, vomiting, nausea, oral discomfort, back, neck or jaw pain, pain in extremity, musculoskeletal discomfort, hyperhidrosis, malaise, and asthenia. See SPC for details of other undesirable effects. Presentation: One carton contains a single vial of Rapiscan (400 micrograms regadenoson in 5mL solution for injection). Price: Please see your local distributor. ATC code: C01EB21. Legal Classification: UR. Marketing authorization holder: Rapidscan Pharma Solutions EU Ltd, Regent's Place, 338 Euston Road, London, NW1 3BT, United Kingdom. Marketing authorization number: EU/1/10/643/001 Date of preparation: April 2012.

IDB Holland is the exclusive distributor in The Netherlands

IDB Holland bv
Weverstraat 17
5111 PV Baarle-Nassau
The Netherlands

Phone: +31 (0)13 507 9558
Fax: +31 (0)13 507 9912
E-mail: sales@idb-holland.com
Internet: www.idb-holland.com

Date of preparation: April 2012 RPS EU 12-009

For more information please visit **www.rapiscan-mpi.com**

Oorspronkelijke data

In deze uitgave van ons Tijdschrift vindt u maar liefst twee artikelen waarin oorspronkelijke bevindingen gepresenteerd en bediscussieerd worden. Het publiceren van artikelen met oorspronkelijke data past in het streven van de redactie om de goede kwaliteit van ons Tijdschrift te waarborgen.
Conform de richtlijnen van de European Association of Nuclear Medicine (EANM) wordt op de meeste afdelingen Nucleaire Geneeskunde ^{18}F-FDG toegediend in een dosis die lineair evenredig is met het gewicht van de patiënt. De beeldkwaliteit is echter niet alleen afhankelijk van de toegediende dosis, maar ook de gevoeligheid van de camera - moderne PET camera's hebben een hogere gevoeligheid dan oudere systemen- en het gebruikte acquisitieprotocol spelen een belangrijke rol. In het eerste artikel met oorspronkelijke data vroeg Wientjes zich dan ook af of de FDG dosis, als een moderne PET scanner wordt gebruikt, wel lineair evenredig moet zijn met het gewicht van de patiënt, en zij komt met verrassende antwoorden.
Adenosine wordt regelmatig toegediend bij myocardperfusie scintigrafie. Vele lezers kunnen zo een lijstje opdreunen van bijwerkingen van adenosine, zoals verminderde prikkelgeleiding via de atrioventriculaire knoop en hoofdpijn. Bovendien kunnen patiënten soms niet optimaal fysiek ingespannen worden of zijn er contra-indicaties voor toediening van adenosine of dobutamine. Regadenoson is een selectieve adenosine-2A receptor agonist. Regadenoson geeft na toediening een snelle vasodilatatie en zou minder bijwerkingen induceren dan adenosine. In het tweede artikel met oorspronkelijke data van deze uitgave induceerde collega Jager vasodilatatie, door adenosine of regadenoson toe te dienen, bij 123 patiënten die verwezen werden voor myocardperfusiescintigrafie. Jager bestudeerde of de afwijkingen die gezien werden op het scintigram vergelijkbaar waren tussen beide groepen, en of regadenoson minder bijwerkingen gaf dan adenosine.
Collega Noordzij beschrijft een interessant geval, waarin de resultaten van ^{18}F-FDG PET onderzoek de oorzaak konden aangeven van een zeldzame complicatie van een coloscopie: een gastrocolocutane fistel.
Recentelijk bereikte ons de berichten dat Marian Plaizier en Peter van Urk zijn overleden. Marian is overleden op 23 mei 2013. Zij is maar 48 jaar geworden. Marina werkte als Nucleair Geneeskundige in Tilburg. Namens de redactie wensen wij haar nabestaanden heel veel sterkte toe in deze moeilijke tijd.
Peter is op 2 mei 2013 overleden. Hij was bestuurslid van de Nederlandse Vereniging voor Nucleaire Geneeskunde (NVNG) van 1981 tot 1988, waarvan de laatste drie jaar als voorzitter. Van 1990 tot 2010 was hij redactielid van ons Tijdschrift. In die periode was hij ook enige tijd hoofdredacteur. Met dankbaarheid denken we terug aan de vele bijdragen die hij aan de ontwikkeling van de Nucleaire Geneeskunde heeft geleverd.

Jan Booij
Hoofdredacteur

Voorblad: opname van ^{11}C-docetaxel in longcarcinoom (met dank aan Dr. A.A.M. van der Veldt en A. Reniers).

Body mass independent ^{18}F-FDG PET image quality; implementation of a power law based dosage regime

R. Wientjes, MSc[1,2], D. Dickerscheid, PhD[1], J. Lavalaye, MD PhD[3], J.B.A. Habraken, MSc[1]

[1]*Department of Medical Physics, St. Antonius Hospital, Nieuwegein, The Netherlands*
[2]*Department of Medical Technology and Clinical Physics, University Medical Center Utrecht, The Netherlands*
[3]*Department of Nuclear Medicine, St. Antonius Hospital, Nieuwegein, The Netherlands*

Abstract

Wientjes R, Dickerscheid D, Lavalaye J, Habraken JBA. Body mass independent ^{18}F-FDG PET image quality; implementation of a power law based dosage regime. Most European hospitals have implemented a linear dosage regime in line with the EANM guidelines for the administration of ^{18}F-FDG. Thus, the administered dose is proportional with the body mass of the patient. With such a linear administration procedure the image quality deteriorates with increasing body mass. The required amount of ^{18}F-FDG per unit of body mass to acquire a PET scan of sufficient diagnostic quality depends among others on the sensitivity of the scanner, the acquisition protocol and the reconstruction algorithm. In anticipation of a proposal of the Dutch society of nuclear medicine for the adoption of the EANM guidelines, which provides flexibility to adapt the ^{18}F-FDG admission to the improved sensitivity of new scanners, we found that for the scanner that we use the minimum amount of ^{18}F-FDG required to meet the minimum image quality criteria was equal to 4 MBq·min/kg. However, implementing this dose-scheme would result in a suboptimal image quality for patients with higher body masses. To correct for this, we retrospectively analysed data from fifty patients, who received a dose linear to their body mass, to construct a model of the image quality and body mass. Image quality was defined here as the signal to noise (SNR) ratio in the liver. The observed relation between body mass and image quality and the desired signal to noise ratio of the liver resulted in a power law based regime. Before implementing this regime in clinical practice, we first tested it by a posteriori reconstructing data of patients recorded in list mode to simulate its effects. The new regime was finally evaluated after the implementation in the clinical practice.
The new dosage regime provided good image quality independent of the body mass. On average, the amount of ^{18}F-FDG used was 17% lower compared to the former dosage regime. **Tijdschr Nucl Geneesk 2013; 35(2):1048-1052**

Introduction

In most positron emission tomography (PET) centres the dosage of ^{18}F fluordeoxyglucose (FDG) administrated to patients is linearly to the body mass of the patient. For obese patients such a linear dosage protocol can lead to noisy images that might be hard to interpret diagnostically and a higher dosage in these cases is desirable. For paediatric and underweight patients, however, the same linear dosage protocol leads to excellent images but, arguably, a higher dose is administered than strictly necessary to achieve the required diagnostic image quality.

The image quality of an ^{18}F-FDG PET scan depends, among others, on the injected activity, the body mass, the sensitivity of the PET scanner, and the acquisition protocol (time per bed position).

The current guideline of the European Association of Nuclear Medicine (EANM) prescribes the amount of activity (in MBq) to be injected in terms of the product of the ratio between injected dose and body mass and the time per bed position (MBq/kg·min/bed). This product should be larger than a given value, which depends on the type of PET scanner and is specified in the guideline (1).
The guideline of the EANM does not yet take into account the high sensitivity of the new generation of PET scanners as well as other features, such as time-of-flight (TOF) and point-spread-function (PSF) reconstruction capabilities. As a result the necessary amount of activity to be injected to satisfy the guidelines if one used one of the new PET scanners is higher than strictly necessary for patients with a normal body mass.

This has been acknowledged and an update of the EANM guideline for the Netherlands has been proposed (2). In the proposed update, the minimum activity concentration of ^{18}F-FDG needs to be such that the image quality of acquisitions satisfies certain minimal conditions as specified for the National Electrical Manufacturers Association (NEMA) NU2-2001 Image Quality phantom (1,2). The image quality is characterised here by the coefficient of variance (COV) and the recovery coefficient (RC), which correspond to the measure of the noise level in a known homogeneous

background and the ratio of the measured versus the true contrast (1), respectively.

The quality of PET images is always limited in obese patients because of the prominent photon attenuation and high scatter fractions resulting in an increased image noise (3, 4). In a previous issue published in this journal, Van Dalen *et al* (5) presented a method to determine the optimal dose to be injected as a function of body mass by retrospectively measuring the noise level in PET/CT data. Van Dalen *et al* found that for their PET scanner and reconstruction parameters the optimal activity depended on the body mass of the patient through an approximately quadratic power law.

In spite of these encouraging results the power law based dosage regime has not been generally adopted in clinical practice and, to the best of our knowledge, there have been no publications of a successful implementation.

The main goal of this work was to apply and validate the method of Van Dalen and co-workers to our PET scanner and reconstruction parameters.

Material and methods

This study was performed using a Philips Gemini TF-64 PET/CT scanner (2010). The PET scans were acquired using the linear dosage regime (2.3 MBq/kg) and a scan time of 2.5 min/bed for the thorax and abdomen and 2 min/bed for the bed positions of the lower extremities.

For image reconstruction we used the scanners default line of response/time-of-flight/ordered subset expectation maximisation (LOR/TOF/OSEM) reconstruction algorithm with 33 subsets, 3 iterations. The low dose CT (64 slice) based attenuation correction was acquired with 120 kV and 50 mAs/slice for patients with a body mass index below 35 and 80 mAs/slice otherwise.

Determining the reference dose

To determine the minimum dose that still satisfied the criteria proposed by Boellaard *et al* (2) we first performed measurements with the NEMA IQ phantom for various values of the product MBq/kg·time/bed. From the reconstructed images we determined the minimal FDG activity for which the COV and RC still satisfied the updated guidelines (2). Because the IQ phantom is a representative model for a patient of 75 kg body weight, we used the result of our phantom measurements as a reference dose within the model that we derived from the analysis of our patient data.

Clinical data analysis

We retrospectively selected 50 clinical patients who received an FDG PET/CT examination without the use of contrast agents after March 1st 2012. Patients with reported liver disease or abnormalities in the liver were excluded from our selection. Special care was taken to ensure that in our selection of patients a broad range of body masses was represented (average 77 kg body weight, range 50 – 109 kg).

After an intravenous administration of 2.3 MBq/kg of ^{18}F-FDG and a waiting time of 60 minutes in accordance with the EANM guidelines (1), all patients were scanned using a scan time per bed position (T_{bed}) of 2.5 minutes for the abdominal region (5.75 MBq·min/kg). Each patient dose was prepared manually at the radiochemistry laboratory of our institution and the calibration times were chosen to coincide with the planned administration times.

To characterise the image quality of the patient data we used the signal-to-noise ratio (SNR) in the liver (3). The SNR was determined as follows; On the CT data, we first visually determined the slice where the cross section of the liver was largest. On this slice and on the two adjacent slices an oval region of interest (ROI) was drawn. The ROIs were drawn as large as possible while keeping a safe margin from the edge of the liver to ensure that only counts originating from the liver were included. For each of the three ROIs we determined the average pixel value and the standard deviation and successively the SNR which was defined as the ratio of the average pixel value and the standard deviation. Finally, we defined SNR_{liver} as the average of the three SNR values (3).

For each patient we recorded the injected activity (A[MBq]), the calibration time of the activity, the time of administration, the starting time of the PET scan, and the patient reported body mass (M[kg]). Unless explicitly stated all the activities mentioned have been determined at T=-1 h, where T=0 h is the starting point of the scan.

In the desired situation, the image quality and therefore the value of SNR_{liver} does not depend on the body mass of the patient. To arrive at a dosage regime in which the image quality is independent of body mass, we first need to determine the relationship between body mass, injected activity, and SNR_{liver}. The SNR is roughly inversely proportional to the square root of the activity (5). To compensate for this effect we scaled the SNR_{liver} data with the square root of the (injected) activity $SNR_{liver}' = \sqrt{SNR_{liver}}$.

To determine the relation between body mass (M[kg]) and image quality we fitted the SNR_{liver}' data as follows; $SNR_{liver}' = a \cdot M[kg]^b$, where a and b are fitting parameters. After substituting the definition of SNR_{liver}' into this equation we arrive at an explicit dosage regime in which the image quality is independent of body mass;

$$A[MBq] \cdot T_{bed}\,[\text{min}] = \left(\frac{SNR^*}{a}\right) \cdot M[kg]^{-2b} \qquad (1)$$

where SNR_{liver} is replaced by SNR* to denote that this is the desired image quality. A value of b = -0.5 corresponds

to a linear equation and b = -1 corresponds to a quadratic relation between body mass and image quality. The value of SNR*, however, cannot be chosen completely arbitrarily. As discussed above the EANM guidelines for PET scanner calibration imply that the image quality of images acquired with the NEMA IQ phantom satisfies certain minimal requirements. The IQ phantom is representative for a patient with a body mass of 75 kg. The minimum requirements are expressed as A[MBq]·T_{bed}[min] at 75 kg. We can explicitly rewrite equation 1 into an equation for the minimum SNR** at 75 kg;

$$SNR^{**} = a \cdot M\,[kg]^{b}\sqrt{A[MBq] \cdot T_{bed}\,[\text{min}]} \qquad (2)$$

The chosen value for the SNR, denoted by SNR*, we derived from the minimal SNR** value that followed from our phantom measurements with an additional margin.

Validation of low dosage regime

For lower body masses, the power law based dosage regime prescribes a lower activity to be injected than the linear dosage regime. For 7 patients with body masses (significantly) lower than 75 kg we reconstructed the list-mode data of the original exam for a shorter acquisition time. The ratio of the reduced acquisition time and the original acquisition time was chosen to be equal to the ratio of the activities in the power law based and linear dosage regimes. In this way it is possible to simulate the effects of the lower activity on the image quality. The resulting images were subsequently reviewed by a nuclear medicine physician and the SNR was determined to verify that the reconstructed data was consistent.

Clinical evaluation of new dosage regime

After the introduction of the power law based dosage regime we repeated the analysis that we used to derive the new dosage regime for our system. We selected the first 50 patients based on the same inclusion criteria. For this group of patients we determined the SNR in the liver and checked if the SNR had become independent of body mass. Finally, we compared the amount of ^{18}F-FDG purchased after the introduction of the new dosage regime to a similar period before the introduction of the dosage regime.

Results

From the analysis of our measurements with the NEMA IQ phantom we found for the acquisition and reconstruction parameters in our institution that the minimum amount of FDG that has to be administered was equal to 4 MBq/kg·min/bed. From this we determined the reference dose for a patient of 75 kg to be 5 MBq/kg·min/bed.
It can be seen from figure 1 that the image quality (SNR_{liver}) decreases with increasing body mass. Figure 2 shows the scaled signal to noise ratio SNR_{liver}' as a function of the body mass using the linear dosage regime. SNR_{liver}' decreases with increasing body mass.

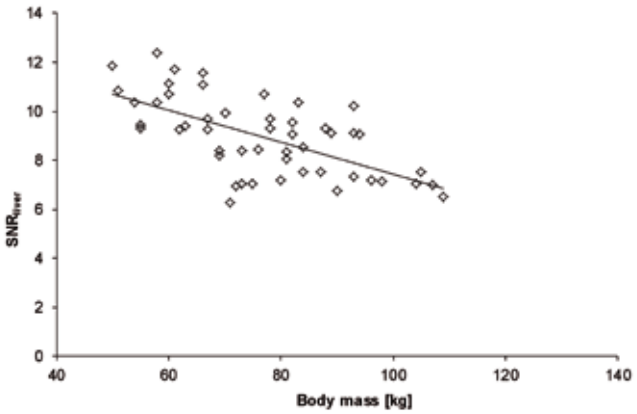

Figure 1. Signal to noise ratio in the liver (SNR_{liver}) versus body mass for 50 patients using the linear dosage regime.

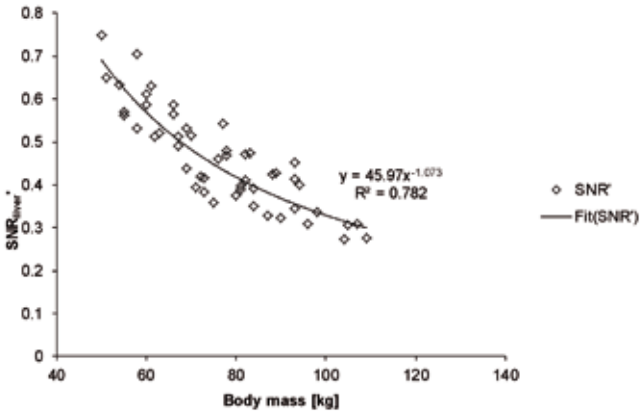

Figure 2. Scaled signal to noise ratio SNR_{liver}' as a function of body mass using the linear dosage regime.

With the result of the fit parameters a and b from figure 2 substituted in equation 2 it follows that the minimum SNR** is equal to 7.8 (with a dose of 4 MBq/kg·min/bed at 75 kg). The chosen value SNR* equals 8.7 (with a dose of 5 MBq/kg·min/bed at 75 kg). For our situation equation 1 reduces to;

$$A[MBq] \cdot T_{bed}\,[\text{min}] = 0{,}036 \cdot M[kg]^{2{,}146} \qquad (3)$$

Our simulation of shorter acquisition times for patients with low body masses shows that, as expected, the image quality deteriorates slightly, SNR_{liver} was 10.2 in the linear regime and 8.9 with the new regime. However the resulting SNR is higher than the expected SNR* (8.32, difference not significant p=0.34).

Table 1. Measured SNR_{liver} of the simulated power law based dosage regime. The reference SNR was set to 8.32.*

body mass [kg]	SNR_{liver} linear dosage regime	SNR_{liver} simulated new dosage regime
47	11.6	9.33
52	8.98	7.91
55	9.00	6.88
55	10.8	8.62
59	10.5	9.83
65	8.59	8.23
66	11.7	11.7
average	10.2	8.9

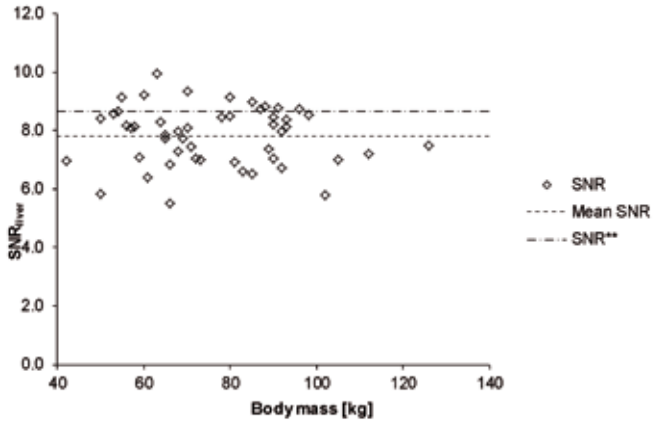

Figure 3. SNR versus body mass after the implementation of the new dosage regime.

Figure 3 shows the SNR_{liver} versus body mass after the introduction of the new dosage regime. We see that the SNR_{liver} has become independent of body mass (Pearsons r= -0.06, p=0.66). The average value of SNR_{liver} is significantly (p<0.01) lower than the reference value (7.8 versus 8.7).

We also compared the amount of ^{18}F-FDG that was used before and after the introduction of the new dosage regime. For 216 patients data were analysed and on average 17% less (p=0.016) ^{18}F-FDG was used with the new dosage regime compared to the linear dosage regime, which has resulted in a significant reduction in operating costs.

Discussion

In this work we have shown how to determine and implement a dosage regime for ^{18}F-FDG PET/CT scans that results in an image quality that is independent of body mass.
Figure 3 shows that image quality as expressed by the SNR_{liver} is independent of body mass. However, the average SNR_{liver} value (7.8) is lower than the chosen reference value SNR* (8.7) and shows a large variance (SD=1.0).
In the following we briefly discuss some of the causes for this difference. Figure 4 shows the relation between the deviation of the planned patient dose at the start time of the scan and the SNR_{liver}.

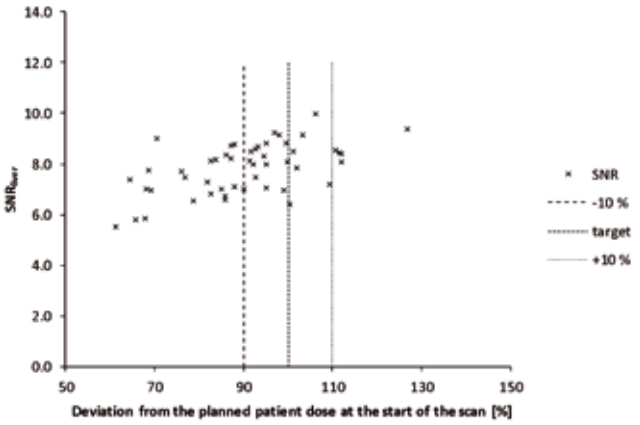

Figure 4. Signal to noise ratio in the liver versus the deviation from the planned patient dose at the start of the scan.

We can see from this figure that the accuracy of the FDG patient dose preparation and variations in the injection and start time of the scan resulted in a deviation from the planned dose which affects the final SNR_{liver}. The EANM guidelines (1) recommend that the prepared patient dose has to be within 10% of the ordered target dose. An analysis of the 50 patient dose preparations, used for the evaluation of the power law based dosage regime, showed that in 43 patients the prepared dose was within 10% of the ordered dose. On average the dose was 2.5% lower than the ordered dose.

Another important parameter that needs to be strictly controlled is the time interval between the injection of the activity and the start of the scan. The EANM guidelines allow for a maximum 5 minute deviation from the 60 minute waiting time in the protocol. In 11 patients the scan was started within 55 to 65 minutes after the calibration time. On average scans started 76 minutes after the calibration time. The calculated activity one hour before the start of the scans was lower than 90% of the desired value in 23 patients. The average amount of ^{18}F-FDG at the start of the scan was 90% of the ordered dose. Deviations in waiting time between administering and start of the scan do not only result in a deviation from the desired activity at the start of the scan, but also lead to unknown deviations in liver uptake.
The reasons for these deviations have been analysed and were due to delays in scheduled program and technical

problems with the PET scanner. Our investigations have led to increased awareness and a stricter adherence to the protocol.

We have not explicitly taken into account the net dose, i.e., the effect of remaining activity in the syringe after injection. For a sample of 12 syringes we found that the residue was on average 1.7% (range 0.3% to 7.5%) of the activity at the moment of administering. The EANM guidelines assume a 1% margin (1). The net activity used for the patient doses in figure 4 where unknown.

It is important to note that body masses used in the analysis were a patient reported outcome. This is not in accordance with the EANM guidelines, therefore we advised the department to adopt this part of the guideline. The two effects (remaining activity and deviations in reported body mass) have direct consequences for the quantification as expressed by the Standard Uptake Value (SUV); The deviation of the body mass from the true body mass and the deviation of ordered activity and the net injected activity are directly proportional to the SUV.

Our analysis is based on an assessment of the SNR based on ROI analysis. To minimise the effect of inter en intra operator variability a single observer has drawn all the ROIs for this study in a protocolled manner.

It should be stressed that the dosage regime derived here only applies to the specific parameters that we use at our institute and should not be copied blindly. For different types of PET scanners and reconstruction parameters the method presented in this work can be used without modification but the resultant dosage regime will probably be different.

Acquisition time versus dose

Because the dose parameter (MBq·T_{bed}) depends both on the injected activity and the duration of the scan there is a choice to be made between increasing the acquisition time (which saves ^{18}F-FDG) or, alternatively, increase the dose (which saves time). Our institute has two FDG preparation rooms where the tracer is administered, which means that reducing the acquisition time will not lead to a higher PET scanner throughput because the preparation rooms will be occupied.
For patients up to 95 kg we use an acquisition time of 2.5 min/bed. Patients with a body mass of more than 95 kg we use 3 min/bed, which saves ^{18}F-FDG (figure 5). On average we see one patient per day who is heavier than 95 kg. The maximum amount of 400 MBq is reached for 129 kg and for higher body masses we accept a lower image quality.

One may argue whether, with increasing dose, the scanner is still used in the linear range of the noise-equivalent count rate (NECR). When this is not the case, only prolonged scan time can improve the image quality (3,4). For the power law based dosage regime that we propose subjects with a body mass of 129 kg or more will, on average, have a FDG concentration of

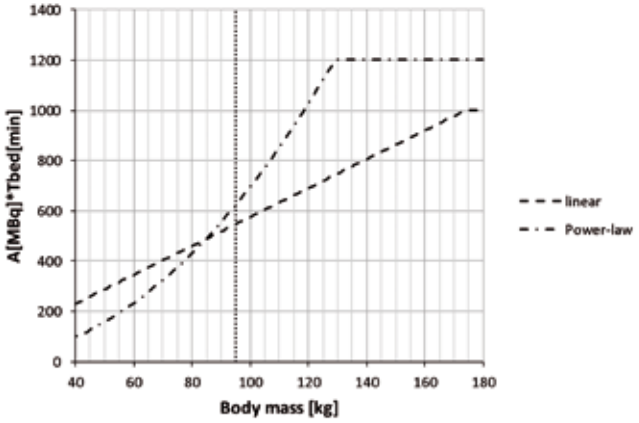

Figure 5. Linear and power law based dosage regime. In the new dosage regime the scan time per bed position increases from 2.5 to 3 minutes when body mass is 95 kg or more. Based on experience a lower cut-off of 30 kg is used.

1.8 kBq/ml one hour pi. This concentration falls within the linear range of the NECR curve of our scanner, even when the NEC rate curve is determined using a 35cm diameter phantom, the maximum of the NEC rate curve in that case is found at 7.5 kBq/ml (6).

Conclusions

We have successfully implemented a power law based dosage regime for ^{18}F-FDG PET/CT scans which has resulted in good image quality that is independent of body mass. An additional benefit of the new dosage regime was a reduction of the total amount ^{18}F-FDG used (17%).
Based on the results of our investigations we successfully implemented a power law dosage regime in our clinical routine.

References

1. Boellaard R, O'Doherty MJ, Weber WA et al. FDG PET and PET/CT: EANM procedure guidelines for tumour PET imaging: version 1.0. Eur J Nucl Med Mol Imaging. 2010; 37:181-200
2. EANM/NL procedure for assessing PET/CT system specific patient FDG dose preparations for quantitative FDG PET studies. www.nvng.nl (restricted area, members only) Accessed: 29th March 2013
3. Halpern BS, Dahlbom M, Auerbach MA et al. Optimizing imaging protocols for Overweight and Obese Patients: A Lutetium Orthosilicate PET/CT Study. J Nucl Med. 2005;46:603-7
4. Masuda Y, Kondo C, Matsuo Y, Uetani M, Kusakabe K. Comparison of imaging protocols for 18F-FDG PET/CT in overweight patients: Optimizing scan duration versus administered dose. J Nucl Med. 2009;50:844-8
5. Dalen JA van, Mulder H, Kamp P et al. Optimizing administered FDG dose for PET imaging. Tijdsch Nucl Gen. 2010;32:433-7
6. Surti S, Kuhn A, Werner ME et al. Performance of Philips Gemini TF PET/CT scanner with special consideration for its time-of-flight imaging capabilities. J Nucl Med. 2007; 48:471-80

Regadenoson as a new stress agent in myocardial perfusion imaging; initial experience in the Netherlands

P.L. Jager, MD PhD[1], M. Buiting, MPA[1], M. Mouden, MD[1,2], A.H.J. Oostdijk, MD[1], S. Knollema, MD PhD[1], J.P. Ottervanger, MD PhD[2]

[1]*Department of Nuclear Medicine, Isala klinieken, Zwolle, The Netherlands*
[2]*Department of Cardiology, Isala klinieken, Zwolle, The Netherlands*

Abstract

Jager PL, Buiting M, Mouden M, Oostdijk AHJ, Knollema S, Ottervanger JP. Regadenoson as a new stress agent in myocardial perfusion imaging; initial experience in the Netherlands. Regadenoson is a new and recently approved agent to induce pharmacological stress in myocardial perfusion imaging (MPI) procedures using a single bolus injection. It is a selective adenosine-2A receptor agonist with rapid onset of coronary vasodilatation of short duration with a favourable side-effect profile. We included 123 patients referred for MPI because of suspected CAD or follow-up of CAD, of whom 66 consecutive patients underwent a regadenoson stress test and 57 consecutive patients underwent an adenosine stress test preceding standard myocardial SPECT imaging. Technologists, physicians and patients were all asked to report their experience using questionnaires, both for regadenoson and adenosine. As compared to adenosine, regadenoson produced fewer AV blocks (0 vs. 10% with adenosine), minor tachycardia, minimal blood pressure changes, while other side effects were milder and shorter as assessed both by the patients themselves as well as technologists and physicians. No medical interventions were required. Patients always considered side effects more severe than medical professionals. Fewer patients had severe complaints on regadenoson than on adenosine (17% and 32%, respectively). The most frequent complaint was dyspnea, followed by flushing and chest pain. When present, these usually disappeared rapidly, but extended beyond 30 min in 10-35% of patients (similar to adenosine). The overall symptom score incorporating presence and duration of side effects was significantly lower after regadenoson than after adenosine (6.7 ± 6.3 and 10.0 ± 7.9, respectively; $P < 0.01$). SPECT imaging results were similar. The regadenoson procedure was faster and more convenient than the adenosine procedure. In conclusion, the selective adenosine-2A selective agonist regadenoson is a new stress agent suitable for myocardial perfusion imaging with a patient- and department friendly profile. **Tijdschr Nucl Geneesk 2013; 35(2):1053-1058**

Introduction

Single photon emission computed tomography (SPECT) myocardial perfusion imaging (MPI) using 99m-technetium (^{99m}Tc) labelled flow tracers such as ^{99m}Tc-sestamibi or ^{99m}Tc-tetrofosmin is one of the cornerstones in the work-up of patients with suspected coronary artery disease (CAD). The method has been around since the eighties of the past century and is mentioned in many guidelines around the world (1). Uptake of these tracers into myocardial tissue has a fairly linear relation with myocardial blood flow. The principle of MPI is the comparison of myocardial activity between a stress and rest acquisition, and is based on decreased tracer uptake in tissue supplied by a stenotic artery as compared to tissue supplied by a normal epicardial artery. The resulting reversible defect between stress and rest is the hallmark of myocardial ischemia.

Various methods exist to produce the stress required for MPI. Conventional bicycle or treadmill exercise is still widely used, and apart from representing normal daily life, it also provides information on a patient's functional capacity. However, as many patients are unable to produce the required level of exercise, pharmacological stress methods with equivalent diagnostic potential have been developed (2). Adenosine, dipyridamol and dobutamine are the most commonly used agents for this purpose. Adenosine and dipyridamol produce a coronary vasodilatation in normal epicardial arteries that decreases in stenotic arteries that are unable to dilate. In this way reversible perfusion defects are again induced, although this is a situation of luxury perfusion as the myocardial demand is not increased. Similar to exercise, dobutamine also increases the myocardial oxygen and flow demand. In the USA in 2006, 56% of all MPI procedures were performed using physical exercise, versus 44% using pharmacological stress, of which 63% used adenosine, 30% used dipyridamol and 7% used dobutamine (3).

MPI using adenosine as stress agent is therefore a very common procedure and we are under the impression that the relative use of adenosine is increasing, not only because more and more patients are unable to exercise but also because of the ease and speed of the adenosine stress procedure. Adenosine is a ribonucleoside and apart from being one of the building blocks

of ribonucleic acid (RNA) and deoxyribonucleic acid (DNA), it is also an important precursor in the energy molecule adenosine triphosphate (ATP), involved in the metabolic pathway of various co-enzymes, and plays a role in the intracellular cyclic adenosine monophosphate (cAMP) signal transduction pathway. Adenosine interacts with adenosine receptors, of which four subtypes have been recognised (table 1).

Table 1. Effects of adenosine receptor subtypes

subtype	physiological process
A1 receptor	AV conduction block
A2A receptor	coronary vasodilatation
A2B receptor	bronchoconstriction
A3 receptor	miscellaneous effects on heart and immune cells

There are several drawbacks in using adenosine to induce myocardial stress. Adenosine interacts with all adenosine receptor subtypes and therefore has a wide spectrum of side-effects including AV block, mild to severe bronchoconstriction, flushing and headache as a result of general vasodilatation. Although these effects are quite short, and reverse rapidly after discontinuation of the adenosine infusion, many patients still find adenosine stress tests an unpleasant procedure. The side effects are also the basis of adenosine's contraindications which include second degree AV block and asthma/COPD-like conditions. Especially the latter are frequently encountered in patients evaluated for coronary heart disease, as they may also produce 'cardiac' symptoms such as chest pain and dyspnea.

These drawbacks of adenosine may be overcome by the new stress agent called regadenoson. This drug has been used in the USA for more than five years and has recently been approved for use in the Netherlands (3-6). Regadenoson is a selective adenosine 2A receptor agonist ligand and therefore theoretically does not produce AV block and bronchoconstriction. In addition, the coronary vasodilatation induced by regadenoson occurs very fast. Therefore, the drug can be given as a bolus injection over 10-20 secs. This is followed by a 10 sec saline flush followed by the radiotracer injection. This is a very convenient and extremely fast procedure (5).

The aim of this study was therefore to obtain initial experience using regadenoson as a new stress agent for MPI, focusing on patient tolerance, patient opinions, side effects and logistic aspects in our high throughput cardiac lab. We used regadenoson instead of adenosine for two weeks in all patients and compared findings with those using adenosine in a subsequent week.

Patients and methods

We included 66 consecutive patients referred for MPI because of suspected CAD or follow-up of CAD. In this group 43 were male (65%), mean age was 62.6 years and this ranged from 41 to 88 years. During two consecutive weeks in early 2012 all patients received regadenoson as stress agent instead of adenosine. Findings were compared with 57 patients (31 males (54%), mean age 64 years, range 34 to 84 years) receiving adenosine during a subsequent week, undergoing the exact same evaluation as the regadenoson group.

Regadenoson stress procedure and evaluation

All patients underwent a one day ^{99m}Tc-tetrofosmin MPI protocol with 4-6 hrs between stress and rest tracer administration. Patients were instructed to refrain from caffeine-containing beverages for at least 24 hours prior to the test. All tests were performed by an experienced nuclear medicine technologist in the presence of an experienced cardiologist or nuclear medicine physician.

Patients were connected to an electrocardiography (ECG) and blood pressure monitor and were in supine position during the test. Patients received a 5 mL slow bolus injection of regadenoson containing a fixed dose of 400 micrograms, over 15 – 20 secs, followed by a saline flush of 10 mL, also lasting approximately 10 secs. Then the ^{99m}Tc-tetrofosmin tracer was injected (standard dose 370 MBq, 500 MBq for patients > 100 kg body weight), followed by another 10 mL saline flush. Afterwards patients were monitored for a maximum of 10 min. In this period heart rate, blood pressure and ECG were monitored continuously and were recorded before the regadenoson injection, and 1 minute and 3-4 minutes after regadenoson injection. During the test patients were continually encouraged to report their sensations that were interpreted by the technologists and the physician. Based on their experience in thousands of patients they graded the severity of the complaint on a scale from 0 (absent), 1 (very mild), 2 (mild), 3 (moderate), 4 (severe) to 5 (very severe complaints requiring medical action). In addition the duration of the complaint was recorded into 3 categories: 0 - 1 minute, 1-5 minutes or >5 minutes. Patients complaints were categorised as flushing sensations, chest pain or pressure, dyspnea, overall feeling of fatigue, nausea and abdominal pain, vertigo, and miscellaneous.

In addition to the evaluation by the technologists and the physician, patients were also asked to report on their complaints themselves. They were given a questionnaire to fill out after the regadenoson procedure during the 45-60 minutes wait time before SPECT image acquisition. In this questionnaire the same symptoms as described above were specifically asked, including severity and duration (0-10 minutes, 10-30 minutes, >30 minutes). After the stress procedure all patients resided in a comfortable waiting room under the supervision of a nurse-assistant.

Statistical comparisons of parameters obtained using regadenoson versus adenosine were performed using Student's t-tests for independent parameters using two-side P values of 0.05 as cut-off for significance.

Adenosine stress procedure and evaluation
Regarding the adenosine stress protocol, patients' preparation was similar to the regadenoson procedure. Adenosine was injected intravenously using a continuous infusion at a rate of 140 µg/kg/min for 6 minutes, with the patient in supine position. A weight-adjusted dose of ^{99m}Tc-tetrofosmin (standard dose 370 MBq, 500 MBq for patients > 100 kg body weight) was injected after 3 minutes of adenosine infusion. Patients scheduled for rest imaging received 740 MBq ^{99m}Tc-tetrofosmin (1000 MBq for patients > 100 kg body weight). The injected doses, the process of monitoring and evaluation by technologists and by the patient him- or herself were identical as described under the regadenoson procedure.

SPECT acquisition
For both stress and rest all SPECT images were acquired 45 – 60 mins after tracer injection. Images were acquired using a conventional gamma camera or with a dedicated cadmium-zinc-telluride (CZT) gamma camera. The conventional gamma camera was a dual-head dedicated cardiac camera (Ventri, GE Healthcare) equipped with a low-energy, high-resolution collimator, a 20% symmetrical window at 140 keV, a 64x64 matrix, and an elliptical orbit with step-and-shoot acquisition at 6° intervals over a 180° arc from 45° anterior oblique to 45° left posterior oblique with 30 steps. All patients were imaged in supine position with arms placed above the head. Acquisition time was 12 minutes for the stress images and 15 minutes for the rest images.

The CZT-based SPECT images were acquired using a multi-pinhole camera (Discovery NM/CT 570c, GE Healthcare) and 19 stationary detectors simultaneously imaging the heart. Each detector contained 32x32 pixelated (2.46 x 2.46 mm) CZT elements. A 20% symmetrical energy window at 140 keV was used. All patients were imaged in supine position with arms placed above the head. Acquisition time was 5 minutes for the stress images and 4 minutes for the rest images.

SPECT image quality was assessed by experienced nuclear medicine physicians and cardiologists, and was subjectively graded as 2=good, 1=reasonable, 0=poor.

Results

All 66 patients who received regadenoson tolerated the drug well, and we did not have to administer any additional medication (e.g., aminophylline, salbutamol, nitroglycerine) during the test.

ECG, blood pressure and heart rate
With regadenoson we did not encounter any AV blocks, while in the adenosine group 6 (out of 57) patients developed episodes of 1st and 2nd degree AV block (P<0.01). ECG changes suggestive for ischemia were observed in one (regadenoson) and two (adenosine) patients only.

Systolic blood pressure increased slightly within the first minute after regadenoson but decreased slightly during the next three minutes, producing a post stress value that was nearly the same as the baseline blood pressure (P = NS). Diastolic blood pressure decreased after regadenoson within one minute and remained stable producing a small overall decrease of 6 mm Hg (SD 21).
In the adenosine group the overall decrease in systolic blood pressure was significantly greater than after regadenoson, but the decrease was still modest (decrease from baseline 9 mm ± 27 mm Hg with adenosine versus increase 1 mm ± 15 mm Hg with regadenoson, P <0.05). The decrease in diastolic blood pressure was similar for adenosine and regadenoson (4 mm and 1 mm, respectively, P = NS).

The maximum heart rate clearly increased from 68 ± 11 to 94 ± 15 4 minutes after using regadenoson, which was slightly more than the increase seen after adenosine (heart rate increase after regadenoson and adenosine 26 ± 10 and 22 ± 11, respectively; P<0.05). The maximum observed heart rate at any time in the regadenoson group was 131/minute, versus 133/minute in the adenosine group.

Complaints
In general side effects with regadenoson were few, mild and short and significantly fewer, milder and shorter as compared to the adenosine group (table 2, figure 1). Both the technologists and the patients themselves came to that conclusion.

The mean number of moderate to severe complaints (graded as 3, 4 or 5) as observed by the technologists and the physician was 0.67 ± 0.83 for regadenoson vs. 1.44 ± 1.50 for adenosine (P <0.001). The number of patients experiencing one or more severe complaints was 11/66 patients (17%) after regadenoson, versus 18/57 patients (32%) in the adenosine group (P < 0.01). This same difference was found in the questionnaires filled out by the patients themselves, but at a higher percentage. After regadenoson 31 patients (45%) considered their symptoms severe, versus 50 patients (76%) after adenosine (P<0.001).

In table 2 a breakdown of side effects is presented. After regadenoson dyspnea was the most frequent complaint, followed by flushing and chest pains. After adenosine flushing was the most commonly observed side-effect, followed by chest pain and dyspnea. Interestingly, the severity of the side effects was considered very mild to mild by the technologists but always more severe by the patients themselves.
The duration of side effects with regadenoson was generally short, and in the vast majority all complaints had disappeared within 30 minutes. In 11, 14, 11, 31, 36, 20 % of the patients who developed flushing, chest pain, dyspnea, headache, tiredness, nausea respectively, these extended beyond 30 minutes according to the patients themselves. Slightly lower numbers were found when evaluated by the technologists. Also with adenosine side effects generally resolved quickly, although 10-20% of the patients reported a duration > 30 minutes.

Table 2. Frequency of side-effects (in %, REG n=66, AD n =57).

stress agent	**REG**	**AD**	**REG**	**AD**
assessed by	*technologist/physician*		*patients themselves*	
flushing	41*	71	61*	83
chest pain	23*	56	45	62
dyspnea	55	50	61	68
headache	11	27	42	49
tiredness	15	26	45	53
nausea	18	32	36	42
dizziness	6	27	39	52
overall symptom score	0.67±0.83*	1.67±1.49	0.97±1.04*	1.67±1.09

REG = regadenoson; AD = adenosine; * denotes P<0.05

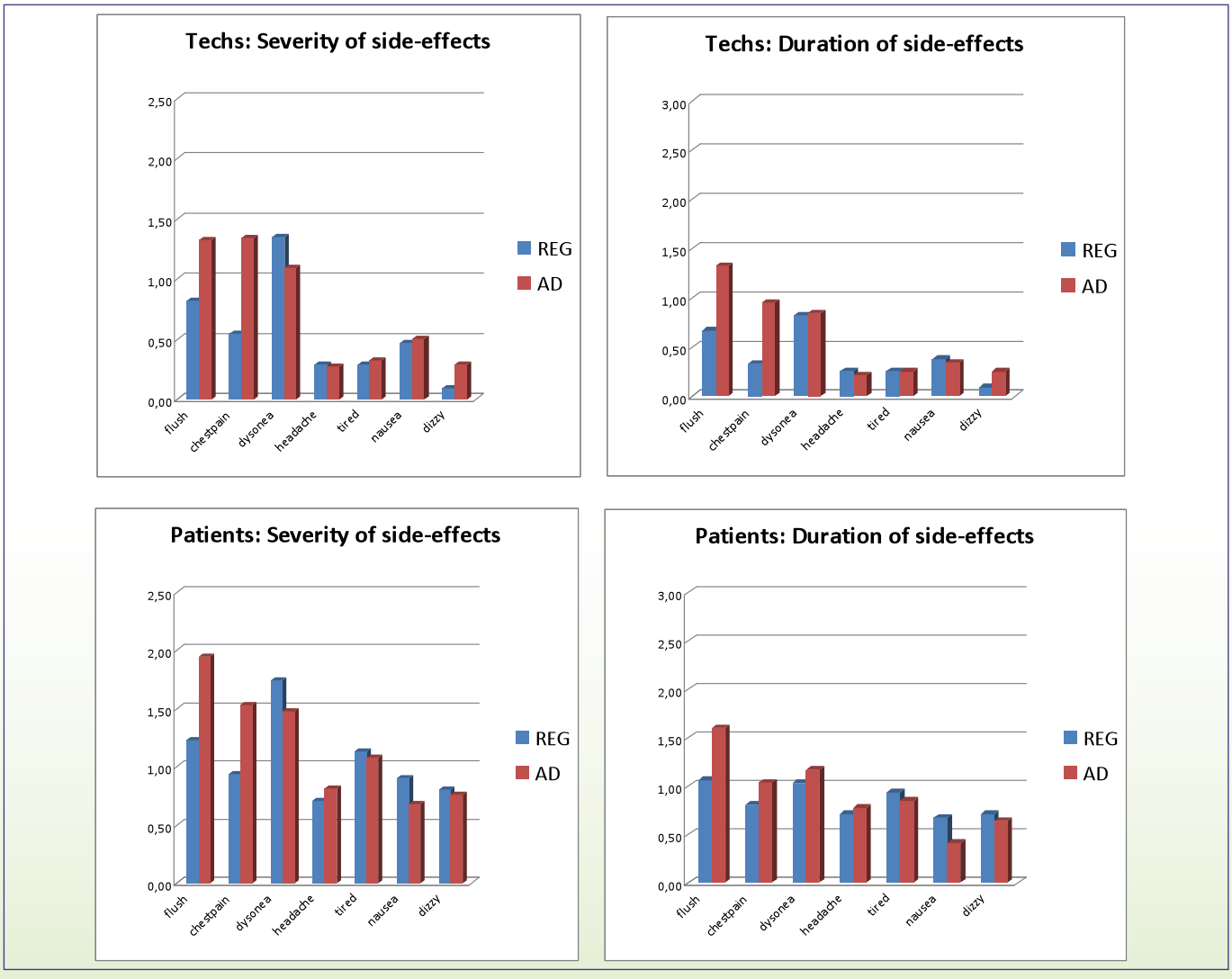

Figure 1. Bar graphs showing severity and duration of side-effects after regadenoson (REG) and adenosine (AD) as assessed by nuclear medicine technologists and patients themselves. Values represent mean values of severity class with range 1 through 5 (very mild, mild, moderate, severe, very severe), and duration class of 0 through 3 (0 absent, 5-10 minutes, 10-30 minutes, >30 minutes).

In order to estimate an overall impression of side-effects we calculated an overall symptom score (defined as the product of severity and duration class, summated for all side effects for each patient). This overall score was significantly lower for regadenoson when compared with adenosine (6.7 ± 6.3 and 10.0 ± 7.9, P < 0.01).

One out of the six patients with known asthma/COPD or on pulmonary medications developed dyspnea (grade 4) but this quickly reversed beginning after one minute. None of the other patients developed any pulmonary symptoms more than grade 1 (very mild).

SPECT results

No difference in final SPECT image quality was noted between both stress agents (mean image quality score 1.91 ± 0.27 and 1.89 ± 0.31, P = NS). SPECT imaging showed ischemia in 14 (21%), fixed defects in 16 (24%) and was considered normal in 39 (59%) in the regadenoson group versus 8 (14%), 11 (19%) and 28 (49%) respectively in the adenosine group.

Logistics

We did not change the scheduled length of the period that patients were present in the stress room (twenty minutes, based on adenosine procedure) and we did not formally measure the time from the beginning to the end of the entire procedure, but it was evident that the regadenoson procedure with its rapid bolus injection and mild side-effect profile was considerably faster and more relaxed for patients and personnel. With adenosine, time is required for preparation of the correct dose, infusion volume and pump, as well as for the six minutes infusion itself, and it usually takes several minutes for symptoms to start reversing before patients can be dismissed from the room. With regadenoson many patients did not have any symptoms at all, and observation for a few minutes after the tracer administration was usually sufficient. Possible late occurring symptoms, after leaving the stress room, were not encountered.

Discussion

Our first experiences with regadenoson in a high throughput nuclear cardiology department were quite positive. As compared to adenosine, fewer patients had side-effects, and if occurring, side effects were milder and of shorter duration as determined both by patients themselves as well as the lab technologists and physicians. SPECT image quality and the ischemia inducing potential were similar. In addition, the procedure was faster and more relaxed.

Regadenoson has been introduced and approved for clinical use in the USA since 2006 and considerable experience has been reported (6-10). In Europe it has only recently been approved. Regadenoson is the first selective adenosine 2A agonist approved by the FDA and is a potent coronary vasodilator with a favourable safety profile that produces few side-effects with a convenient single injection [6]. Although adenosine is also generally well-tolerated its side-effects such as bronchoconstriction and AV blocks can be serious. However, pulmonary symptoms with regadenoson are considerably less and application was safe, as has now been established in several studies (7, 11-13). The affinity of regadenoson for the adenosine 2A receptor is lower than the affinity of adenosine, which induces a relatively short presence at the receptor allowing the use of a single bolus injection, as compared to the need for a constant infusion of adenosine. The abundance of adenosine 2A receptors in the coronary vasculature guarantees a similar maximal vasodilatation effect also for regadenoson as has been established using quantitative PET studies (10).

As expected, our experience aligns with reported results from the USA. We did not experience any AV blocks with regadenoson, effects on blood pressure were minor but a mild regadenoson-induced tachycardia was observed in most patients. With adenosine more AV blocks occurred, effects on blood pressure were slightly more pronounced but tachycardia was slightly milder. Only 1 out of 6 patients (17%) reported one or more severe complaints after regadenoson, whereas adenosine induced almost twice as much. Patients more frequently considered their complaints to be 'severe' after adenosine as compared to regadenoson. The most severe side-effect proved to be dyspnea followed by flushing and chest pain, spontaneously disappearing again in 85-90% within 30 mins. In none of the patients any intervention (bronchodilatation, aminophylline, nitroglycerine) was necessary. In the literature aminophylline has been reported to reverse side-effects rapidly, and some studies even advocate the routine use of aminophylline.

Considerable interest has also been shown in the application of regadenoson at the end of a conventional stress test (e.g., a treadmill test) to further increase the level of stress or to assist in cases where the target heart rate was not reached. This appears to be safe without major adverse events (14, 15). This approach carries the advantage that a patient's functional capacity is also determined, which is not the case with pure pharmacological exercise. In addition, some groups favour the routine use of aminophylline to further reduce side effects (16).
With increasing use of regadenoson the amount of information on safety is increasing. Studies have demonstrated safety of its application in end-stage renal disease and in liver disease (17, 18). Age, gender, obesity and diabetes appeared not to be associated with differences in its safety profile (19). There are case reports that have described acute myocardial infarction during regadenoson stress, likely as a result of steal effects in myocardial blood flow (20). Also epileptic seizures have been described likely associated with regadenoson (21).

The limitations of this study include its small size, non-blinded and non-randomised approach and the limited number of patients with pulmonary disease. However, there is no reason why American patients would respond differently than European patients obviating the need for renewed large studies in Europe.

Another limitation was our two-group comparison, rather than an intra-individual comparison where the same patients would have been stressed both with adenosine and regadenoson.

The most important drawback of regadenoson seems to be the costs. Although regadenoson is not very expensive it is difficult to compete with adenosine, that is locally produced by many Dutch hospital pharmacies for only a few euros per patient. However, the higher cost of regadenoson may be offset by increased patient comfort and possible gains in efficiency as a result of higher throughput and shorter stress times. Another sensible application would be to use regadenoson for patients who cannot undergo adenosine stress testing because of severe COPD or asthma. In this way dobutamine stress with its side-effects and long duration may be avoided. Several Dutch hospitals have started such protocols. Based on multiple literature reports this application appears safe, but more experience is needed (7, 11-13).

Conclusion

In conclusion, the selective adenosine 2A selective agonist regadenoson is a new stress agent suitable for myocardial perfusion imaging with a patient and department friendly profile.

References

1. EANM/ESC procedural guidelines for myocardial perfusion imaging in nuclear cardiology. Available at: http://www.eanm.org/publications/guidelines/gl_cardio_myocard_perf.pdf *Eur J Nucl Med Mol Imag.* 2005;32.
2. Gupta NC, Esterbrooks DJ, Hilleman DE, Mohiuddin SM. Comparison of adenosine and exercise thallium-201 single-photon emission computed tomography (SPECT) myocardial perfusion imaging. The GE SPECT Multicenter Adenosine Study Group. J Am Coll Cardiol. 1992;19:248-57
3. Arlington Medical Resources. Market analysis myocardial perfusion scintigraphy 2006. Available at www.amr-data.com.
4. Al-Jaroudi W, Iskandrian A. Regadenoson: A new myocardial stress agent. J Am Coll Cardiol. 2009;54:1123-30
5. Rapiscan (regadenoson). Summary of Product Characteristics, RPS EU, London.
6. Iskandrian AE, Bateman TM, Belardinelli L, et al; ADVANCE MPI Investigators. Adenosine versus regadenoson comparative evaluation in myocardial perfusion imaging: results of the ADVANCE phase 3 multicenter international trial. J Nucl Cardiol. 2007;14:645-58
7. Thomas GS, Tammelin BR, Schiffman GL, et al. Safety of regadenoson, a selective adenosine A2A agonist, in patients with chronic obstructive pulmonary disease: A randomized, double-blind,placebo-controlled trial (RegCOPD trial). J Nucl Cardiol. 2008 May-Jun;15(3):319-28
8. Mahmarian JJ, Cerqueira MD, Iskandrian AE, et al. Regadenoson induces comparable left ventricular perfusion defects as adenosine: a quantitative analysis from the ADVANCE MPI 2 trial. JACC Cardiovasc Imaging. 2009;2:959-68
9. Kwon DH, Cerqueira MD, Young R, et al. Lessons from regadenoson and low-level treadmill/regadenoson myocardial perfusion imaging: initial clinical experience in 1263 patients. J Nucl Cardiol. 2010;17:853-7
10. Goudarzi B, Fukushima K, Bravo P, Merrill J, Bengel FM. Comparison of the myocardial blood flow response to regadenoson and dipyridamole: a quantitative analysis in patients referred for clinical 82Rb myocardial perfusion PET. Eur J Nucl Med Mol Imag. 2011;38:1908-16
11. Leaker BR, O'Connor B, Hansel TT, Barnes PJ, Meng L, Mathur VS, Lieu HD. Safety of regadenoson, an adenosine A2A receptor agonist for myocardial perfusion imaging, in mild asthma and moderate asthma patients: a randomized, double-blind, placebo-controlled trial. J Nucl Cardiol. 2008;15:329-36
12. Prenner BM, Bukofzer S, Behm S, Feaheny K, McNutt BE. A randomized, double-blind, placebo-controlled study assessing the safety and tolerability of regadenoson in subjects with asthma or chronic obstructive pulmonary disease. J Nucl Cardiol. 2012;19:681-92
13. Husain Z, Palani G, Cabrera R, et al. Hemodynamic response, arrhythmic risk, and overall safety of Regadenoson as a pharmacologic stress agent for myocardial perfusion imaging in chronic obstructive pulmonary disease and bronchial asthma patients. Int J Cardiovasc Imaging. 2012;28:1841-9
14. Aljaroudi WA, Alraies MC, Cerquiera MD, Jaber WA. Safety and tolerability of regadenoson in 514 SPECT MPI patients with and without coronary artery disease and submaximal exercise heart rate response. Eur J Nucl Med Mol Imaging. 2013;40:341-8
15. Parker MW, Morales DC, Slim HB, et al. A strategy of symptom-limited exercise with regadenoson-as-needed for stress myocardial perfusion imaging: A randomized controlled trial. J Nucl Cardiol. 2013;20:185-96
16. Doukky R, Morales Demori R, Jain S, et al. Attenuation of the side effect profile of regadenoson: a randomized double-blinded placebo-controlled study with aminophylline in patients undergoing myocardial perfusion imaging. "The ASSUAGE trial". J Nucl Cardiol. 2012;19:448-57
17. Ananthasubramaniam K, Weiss R, McNutt B, et al. A randomized, double-blind, placebo-controlled study of the safety and tolerance of regadenoson in subjects with stage 3 or 4 chronic kidney disease. J Nucl Cardiol. 2012;19:319-29
18. Aljaroudi W, Iqbal F, Koneru J, Bhambhvani P, Heo J, Iskandrian AE. Safety of regadenoson in patients with end-stage liver disease. J Nucl Cardiol. 2011;18:90-5
19. Cerqueira MD, Nguyen P, Staehr P, Underwood SR, Iskandrian AE; ADVANCE-MPI Trial Investigators. Effects of age, gender, obesity, and diabetes on the efficacy and safety of the selective A2A agonist regadenoson versus adenosine in myocardial perfusion imaging integrated ADVANCE-MPI trial results. JACC Cardiovasc Imaging. 2008;1:307-16
20. Shah S, Parra D, Rosenstein RS. Acute myocardial infarction during regadenoson myocardial perfusion imaging. Pharmacotherapy. 2013 Mar 7. doi: 10.1002/phar.1238. [Epub ahead of print]
21. Page RL 2nd, Spurck P, Bainbridge JL, Michalek J, Quaife RA. Seizures associated with regadenoson: a case series. J Nucl Cardiol. 2012;19:389-91

Gastrocolocutaneous fistula – detected by ^{18}F-FDG PET/CT - as a rare iatrogenic complication of colonoscopy

W. Noordzij, MD[1], R.H.J.A. Slart, MD PhD[1], C.J. Zeebregts, MD PhD[2], A.W.J.M. Glaudemans, MD[1]

[1] Department of Nuclear Medicine and Molecular Imaging University of Groningen, University Medical Center Groningen, The Netherlands
[2] Department of Surgery, Division of Vascular Surgery University of Groningen, University Medical Center Groningen, The Netherlands

Abstract

Noordzij W, Slart RHJA, Zeebregts CJ, Glaudemans AWJM. Gastrocolocutaneous fistula – detected by ^{18}F-FDG PET/CT - as a rare iatrogenic complication of colonoscopy. Colonoscopy is frequently performed in patients with suspected malignancies and inflammatory bowel diseases. It is generally considered to be a low risk procedure. The development of a gastrocolocutaneous fistula is a very rare complication of a perforation during an endoscopic procedure. In case of a patient with fever, abdominal pain and fluid discharge with a history of laparotomy because of perforation during colonoscopy, a fistula should be high in the differential diagnosis. An ^{18}F-FDG PET/CT scan has high diagnostic accuracy for identifying infection and inflammation, and therefore has high potential to visualise fistulas. We describe the first case of a patient who developed a gastrocolocutaneous fistula after a complicated colonoscopy, in which the ^{18}F-FDG PET/CT identified the exact course of the fistula.
Tijdschr Nucl Geneesk 2013; 35(2):1059-1061

Introduction

Colonoscopy is frequently performed in patients with suspected malignancies and inflammatory bowel diseases (Crohn's disease and ulcerative colitis). It is generally considered to be a low risk procedure. Abdominal pain, flatulence, and diarrhoea are among the most common reported complications (1). With an incidence of < 1.0%, the risk of iatrogenic perforation during diagnostic colonoscopy is very low (2,3). The risk of perforation increases up to three times when colonoscopy is combined with therapeutic procedures.

The development of a gastrocolocutaneous fistula is a very rare complication of a perforation during an endoscopic procedure. Only a few cases are known to report this complication after a percutaneous endoscopic gastrostomy (PEG) (4,5). To the best of our knowledge a gastrocolocutaneous fistula has not yet been reported after colonoscopy.

Case report

We present a case of a 48-year-old male who was referred for an ^{18}F-fluorodeoxyglucose positron emission tomography (^{18}F-FDG PET) because of fever, abdominal discomfort and pyogenic discharge from his abdominal wall. Nine months earlier, this patient suffered from intermittent claudication and necrosis of the fifth digit of his left foot, due to a stenosis of his left common iliac artery (CIA). He underwent an amputation of his fifth toe as well as percutaneous transluminal angioplasty of the left CIA, with placement of an endovascular graft. Afterwards, recovery was complicated by a wound infection at the amputation site, for which he underwent another surgical incision with debridement. He was treated with ciprofloxacin and clindamycin.

One month later, he was admitted at the emergency ward because of pain in the right lower abdomen. Abdominal ultrasound showed irritation of the terminal ileum, either due to a terminal ileitis or acute appendicitis. The patient underwent laparotomy, in which an inflamed cecum was found and an ileocecal resection with end-to-side anastomosis was performed. Pathologic analysis showed pseudomembranous colitis, with a positive polymerase chain reaction for Clostridium dificile. Ten days after the laparotomy, a colonoscopy was performed during which biopsies were taken. Histopathology of these biopsies lead to the suspicion of Crohn's disease. After colonoscopy he developed abdominal pain due to an iatrogenic perforation at one of the biopsy sites. Conventional chest X-ray showed free air in the abdominal cavity. The patient underwent re-laparotomy and a subtotal colectomy was performed. Eventually, he received a permanent ileostomy. Afterwards, he was transferred to the intensive care unit (ICU).

At the ICU he again developed a wound infection, this time at the wound site of his laparotomy. Computed tomography (CT) of the abdomen was performed and showed large intra-abdominal fluid collections due to abscesses. A drain was inserted in the fluid collection in the left lower abdomen. Furthermore, he was treated with wide-spectrum penicillin

and recovered rapidly. He was discharged from the hospital two months after his first operation (the amputation of his fifth digit).

During follow up at the outpatient clinic, three months after the discharge, the patient was still recovering. He still suffered from abdominal discomfort. Furthermore, the wound from the latest laparotomy was still leaking fluid. A new CT scan was performed and showed an unspecified fluid collection from the greater curvature of the stomach towards the left lower abdomen, with also an air containing branch towards the anterior abdominal wall. The left external iliac artery containing the stent seemed to be involved in lower abdominal mass. Because the patient also suffered from fever, a combined ^{18}F-FDG PET with low dose CT scan was made to exclude an infection of the endovascular prosthesis in the left common iliac artery.

^{18}F-FDG PET/CT (figure 1 and 2) showed a large fistula originating from the greater curvature of the stomach, towards the ileum, with a branch towards the anterior abdominal wall, as well as a branch towards the descending part of the colon. Neither the endovascular prosthesis in the left communic iliacal artery nor the tissue surrounding it showed elevated uptake, so there was no suspicion of involvement of the endovascular prosthesis. Gastroduodenal endoscopy was performed and showed some mucosal erythema, but no ulcerations or erosive lesions. Biopsies were taken and the material showed one small focus of colon type

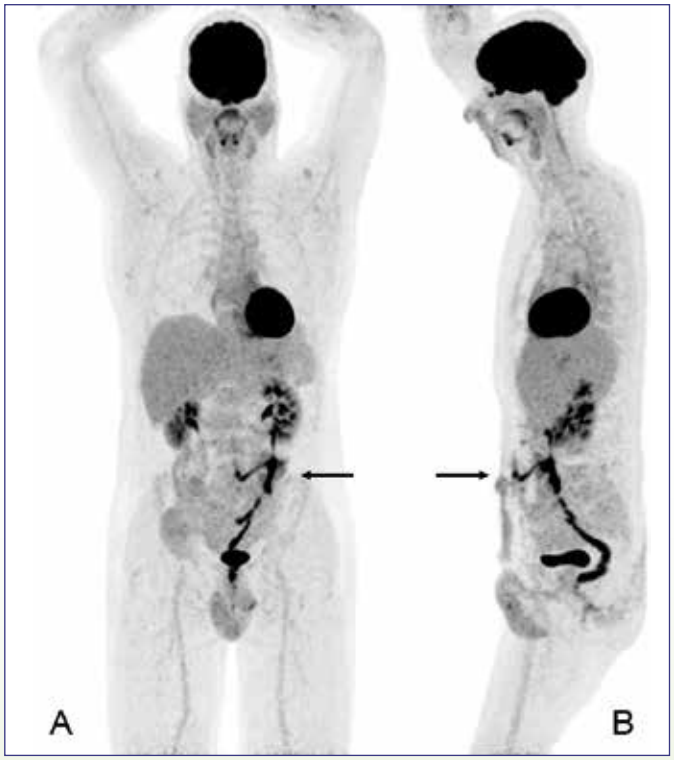

Figure 1. ^{18}F-fluorodeoxyglucose (^{18}F-FDG) positron emission tomography (PET) images in maximum intensity projection scaling (MIP). Coronal (A) and sagittal (B) images show high tracer uptake in the left lower part of the abdomen, indicating the gastrocolocutaneous fistula. The black arrow indicates the level of the cutaneous branch. The images show physiological tracer uptake in the brain, salivary glands, myocardium, liver and spleen, kidneys, digestive tract and the colostomy in the right lower abdomen.

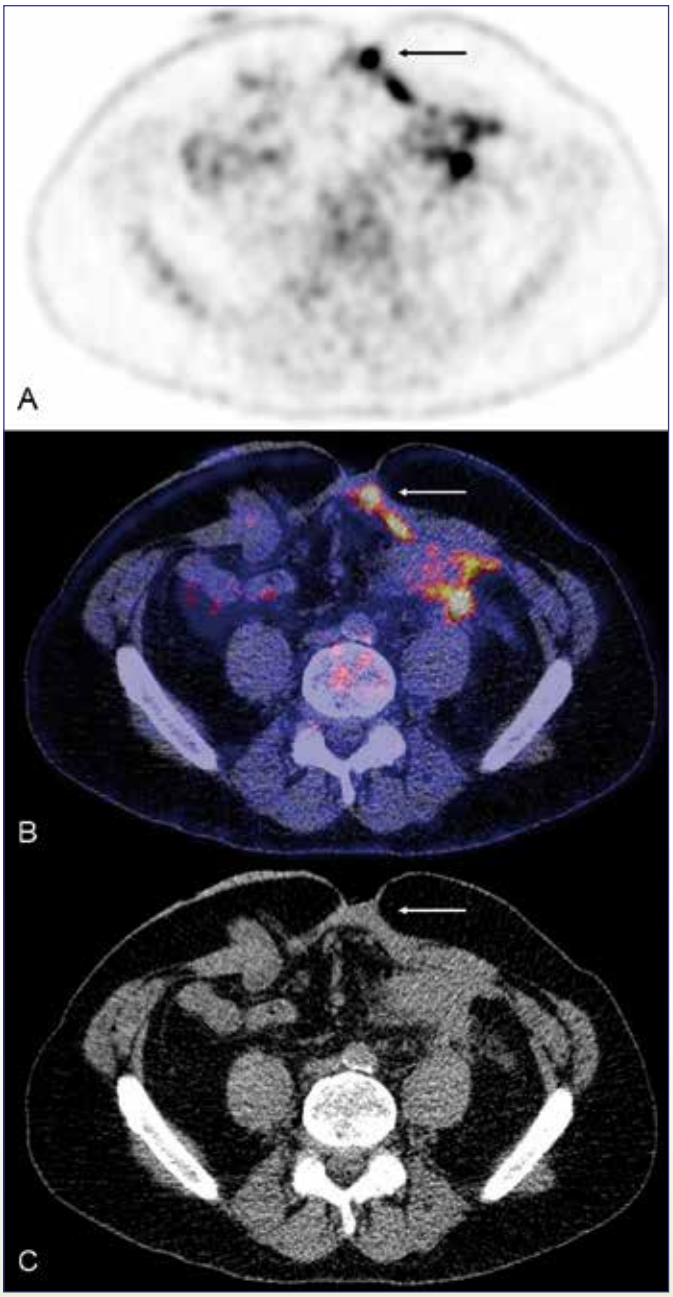

Figure 2. Transaxial image at the level of the black arrow in figure 1. Positron emission tomography image (A, PET), fused image of PET with computed tomography (B, PET/CT), and low dose CT only (C), showing the cutaneous terminus of the gastrocolocutaneous fistula (arrow).

mucosa, with low-grade chronic inflammation surrounding it. The fistula was treated conservatively. One month after the ^{18}F-FDG PET/CT, the discharge was rapidly decreasing, but not completely disappeared.

Discussion

To the best of our knowledge this is the first time a gastrocolocutaneous fistula due to an iatrogenic perforation during colonoscopy is reported. ^{18}F-FDG PET/CT was able to identify the exact course of this fistula.

^{18}F-FDG is a radiopharmaceutical which can be used in both oncological and infectious diseases. FDG is a glucose analogue which enters the cell through glucose transporters (especially GLUT-1) and is phosphorylated by hexokinase into FDG-6-phosphate (FDG-6-P). Afterwards, FDG-6-P is trapped within the cell, since it cannot be dephosphorylised. When combined with the positron emitter 18-Fluorine, it can be used for imaging.

The role of ^{18}F-FDG PET in malignancies is well established. However, its use in infection and inflammation still lacks the support of evidence based medicine (6). Nevertheless, the use of ^{18}F-FDG has been approved for specific infectious indications as fever of unknown origin, osteomyelitis and other chronic bone infections, inflammatory bowel diseases, vasculitis, and infections of vascular prostheses.

Although infections of vascular prostheses are uncommon, the consequences are potentially dreadful. There is an increasing interest in the use of combined ^{18}F-FDG PET with CT (PET/CT) for this indication. The available literature suggests that hybrid ^{18}F-FDG PET/CT is a useful clinical tool, with better test characteristics than CT alone (7). Furthermore, the CT scan should be used for the exact localisation of the FDG uptake. Combined ^{18}F-FDG PET/CT leads to an increase in the diagnostic accuracy (up to >95%) for detecting infected endovascular grafts (8).

The role of ^{18}F-FDG PET in fistulas, however, is still not well established. This is partly due to the fact that most of these fistulas are incidental findings. In the recent history only a few cases of patients with various forms of fistulas were reported, in which ^{18}F-FDG PET was able to visualise the course of the fistula (9,10). Since its high diagnostic value in infection and inflammation, ^{18}F-FDG PET should also be able to identify fistulas in larger cohorts than solitary cases only.

After the introduction of hybrid PET/CT camera systems, in which PET and CT are sequentially performed, the diagnostic accuracy of this modality increased remarkably. Especially the exact localisation of high ^{18}F-FDG uptake with low dose CT is more effortless. New developments lead to the recent introduction of integrated PET/MRI systems. Despite the fact that these systems mainly focus on oncologic cases, a new role may appear for inflammation detection in the near future.

In conclusion, a gastrocolocutaneous fistula is a rare but important complication of colonoscopy. In case of a patient with fever, abdominal pain and fluid discharge with a history of laparotomy because of perforation during colonoscopy, a fistula should be high in the differential diagnosis. ^{18}F-FDG PET has high diagnostic accuracy for identifying infection and inflammation, and therefore has high potential to visualise fistulas, especially when combined with CT.

A short version of this case report is already published in Endoscopy 2013; 45(S 02): E67-E68.

References

1. Lee SH, Cheong YS. Successful endoscopic repair of an iatrogenic colon perforation during diagnostic colonoscopy. J Am Board Fan Med. 2012;25:383-9
2. Wullstein C, Koppen M, Gross E. Laparoscopic treatment of colonic perforations related to colonoscopy. Surg Endosc. 1999;13:484–7
3. Kavic SM, Basson MD. Complications of endoscopy. Am J Surg 2001;181:319 –32
4. Hwang JH, Kim HW, Kang DH, et al. A case of endoscopic treatment for gastrocolocutaneous fistula as a complication of percutaneous endoscopic gastrostomy. Clin Endosc. 2012;45:95-8
5. Roozrokh HC, Ripepi A, Stahlfeld K. Gastrocolocutaneous fistula as a complication of peg tube placement. Surg Endosc. 2002;16:538-9
6. Glaudemans AWJM, Signore A. FDG-PET/CT in infections: the imaging method of choice? Eur J Nucl Med Mol Imaging. 2010;37:1986-91
7. Bruggink JLM, Glaudemans AWJM, Saleem BR et al. Accuracy of FDG-PET-CT in the diagnostic work up of vascular prosthetic graft infection. Eur J Vasc Endovasc Surg. 2010;40:348-54
8. Spacek M, Belohlavek O, Votrubova J et al. Diagnostics of "non-acute" vascular prosthesis infection using 18F-FDG PET/CT: our experience with 96 prostheses. Eur J Nucl Med Mol Imaging. 2009;36(5):850–8
9. Kim M, Lim MC, Seo SS et al. Unusual 2-[18F]-fluoro-2-deoxy-D-glucose accumulation induced by postoperative intestinocutaneous fistula in the patient with uterine cervical cancer and SLE. Arch Gynecol Obstet. 2009;280:141–4
10. Makis W, Ciarallo A, Laufer J et al. Cholecystocolic Fistula of Crohn Disease Mimics Colon Adenocarcinoma Invasion of Gallbladder on F-18 FDG PET/CT. Clin Nucl Med. 2011;36:119-13

PROEFSCHRIFT

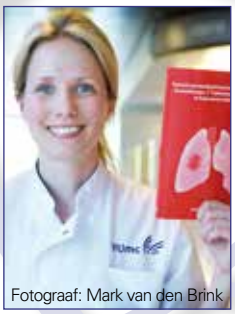
Fotograaf: Mark van den Brink

Dr. A.A.M. van der Veldt

4 juli 2012
VU medisch centrum
Amsterdam

Promotores:
Prof. dr. A.A. Lammertsma
Prof. dr. E.F. Smit

Co-promotores:
Dr. ir. M. Lubberink
Dr. N.H. Hendrikse

Towards personalised treatment planning of chemotherapy: ^{11}C-docetaxel PET studies in lung cancer patients

Met positron emissie tomografie (PET) kan de farmacokinetiek en dynamiek van geneesmiddelen in vivo gevolgd worden. Het gebruik van radioactief gelabelde geneesmiddelen is een veelbelovende techniek om een meer specifieke behandeling voor individuele patiënten met een maligniteit te realiseren. Op de afdeling Nucleaire Geneeskunde & PET Research van het VUmc te Amsterdam is het chemotherapeuticum docetaxel gelabeld met de positron emitter koolstof-11 (^{11}C). In dit proefschrift is de toepasbaarheid van de nieuwe PET tracer ^{11}C-docetaxel bij patiënten met longcarcinoom onderzocht.

PET scans met ^{11}C-docetaxel

Humane whole-body PET computertomografie (PET/CT) scans toonden hoge ^{11}C-docetaxel concentraties in de galblaas en de lever, terwijl de opname in de hersenen en normaal longweefsel laag was (1). Met dynamische PET scans werd vervolgens de opname van ^{11}C-docetaxel in tumoren gekwantificeerd. Daartoe werd eerst het optimale kinetische model ontwikkeld in 34 patiënten met longcarcinoom (2). De netto influx (K_i) van ^{11}C-docetaxel in tumoren was variabel en bleek sterk gerelateerd aan de perfusie. In een kleine groep patiënten, die ook werden behandeld met docetaxel, was een hogere ^{11}C-docetaxel opname in de tumor gerelateerd aan een betere tumorrespons na behandeling met docetaxel.

Microdosis

Aangezien de farmacokinetiek van een microdosis (tracerdosis) ^{11}C-docetaxel en een therapeutische dosis docetaxel verschillend kan zijn, werd ook het concept van microdosering gevalideerd. Daartoe ondergingen patiënten met longcarcinoom, die niet eerder waren behandeld met docetaxel, twee PET scans: één tijdens een bolusinjectie met ^{11}C-docetaxel en een andere tijdens een gecombineerde infusie, bestaande uit ^{11}C-docetaxel en de therapeutische dosis docetaxel. Met de verkregen data van de microdosering scan met ^{11}C-docetaxel kon de opname van docetaxel in tumoren worden voorspeld gedurende de chemotherapie. Na negentig minuten bleek slechts < 1% van de totale therapeutische dosis docetaxel in tumoren te zijn geaccumuleerd.

Effect bevacizumab op ^{11}C-docetaxel opname in tumoren

De vasculaire endotheliale groeifactor (VEGF) komt tot overexpressie op vele maligne tumoren en is een essentiële groeifactor voor de vaatnieuwvorming (angiogenese) van tumoren. Daarom zijn middelen ontwikkeld die de signalering van VEGF remmen. In de klinische praktijk worden angiogeneseremmers vaak gecombineerd met chemotherapie. Een van deze angiogeneseremmers is het humane monoklonale antilichaam bevacizumab. Om het effect van angiogeneseremmers op de opname van chemotherapie in tumoren te evalueren, werd het effect van bevacizumab op de perfusie en opname van ^{11}C-docetaxel in longcarcinoom gemeten. Daartoe ondergingen patiënten verschillende PET scans vóór en na infusie met bevacizumab. Al binnen vijf uur na toediening van bevacizumab namen zowel de perfusie als de opname van ^{11}C-docetaxel in tumoren af (figuur 1). Na vier dagen waren deze effecten nog steeds aanwezig.

Conclusies

De studies in dit proefschrift tonen dat het gebruik van PET scans en radioactief gelabelde geneesmiddelen mogelijk waardevol is om een geïndividualiseerd behandelplan voor patiënten met een maligniteit op te stellen. De studies met ^{11}C-docetaxel in dit proefschrift bieden een goed raamwerk voor de klinische validatie van andere gelabelde geneesmiddelen voor patiënten met een maligniteit. Tenslotte kan worden geconcludeerd dat de effecten van angiogeneseremmers op het transport van chemotherapie naar tumoren verder onderzocht dienen te worden, zodat angiogeneseremmers zo effectief mogelijk kunnen worden ingezet voor de behandeling van patiënten met een maligniteit.

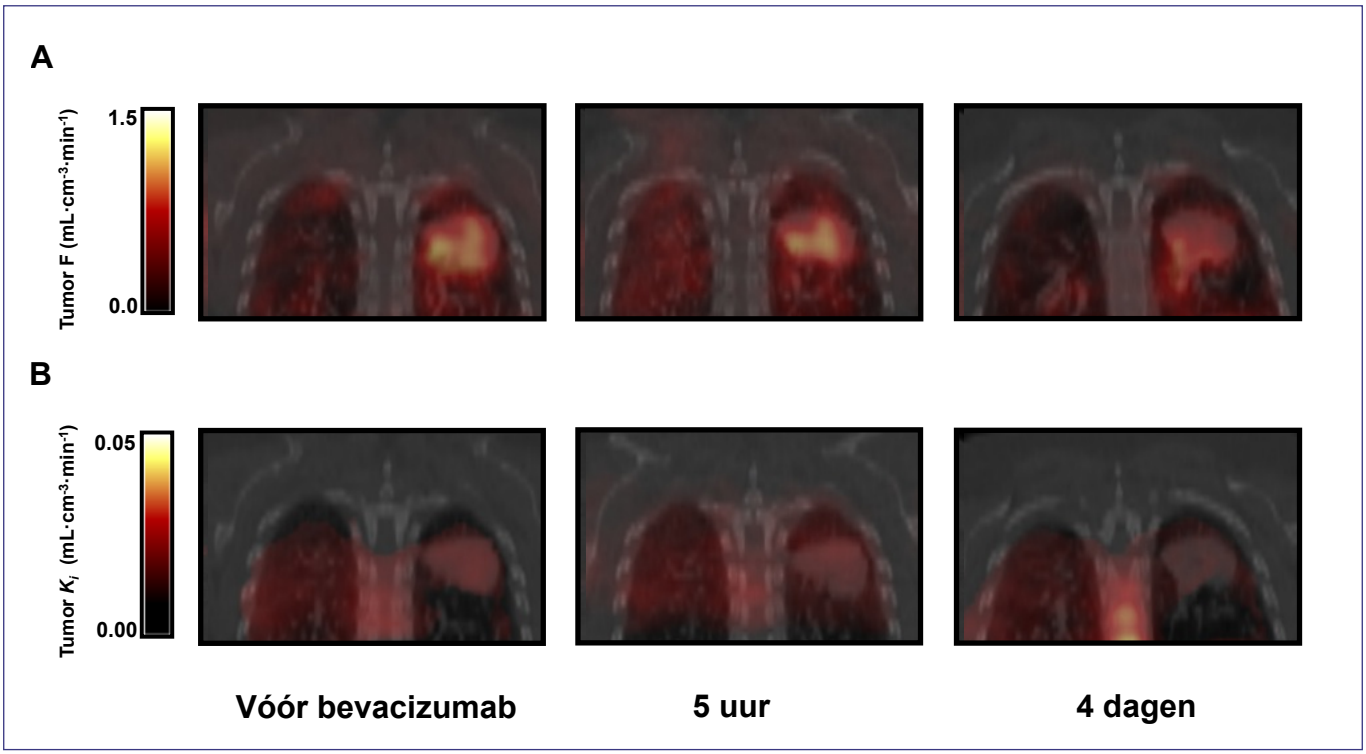

Figure 1. PET/CT scans van een 51-jarige vrouw met een niet-kleincellig longcarcinoom. De PET/CT scans zijn gemaakt voorafgaand aan infusie met bevacizumab en op vijf uur en vier dagen na infusie (3).
A. Parametrische perfusiebeelden (^{15}O-H2O). In de longtumor daalt de gemiddelde perfusie (F) van 0,875 mL·cm^{-3}·min^{-1} vóór infusie met bevacizumab naar 0,765 mL·cm^{-3}·min^{-1} na vijf uur en 0,535 mL·cm^{-3}·min^{-1} op dag vier.
B. PET/CT scans na injectie van ^{11}C-docetaxel. In de tumor daalt de netto influx (K_i) van ^{11}C-docetaxel van 0,0205 mL·cm^{-3}·min^{-1} vóór infusie met bevacizumab naar 0,0193 mL·cm^{-3}·min^{-1} na vijf uur en 0,0127 mL·cm^{-3}·min^{-1} op dag vier.

Literatuur

1. Van der Veldt AA, Hendrikse NH, Smit EF et al. Biodistribution and radiation dosimetry of ^{11}C-labelled docetaxel in cancer patients. Eur J Nucl Med Mol Imaging 2010;37:1950-8
2. Van der Veldt AA, Lubberink M, Greuter HN et al. Absolute quantification of ^{11}C-docetaxel kinetics in lung cancer patients using positron emission tomography. Clin Cancer Res 2011;17:4814-24
3. Van der Veldt AA, Lubberink M, Bahce I et al. Rapid decrease in delivery of chemotherapy to tumors after anti-VEGF therapy: implications for scheduling of anti-angiogenic drugs. Cancer Cell 2012;21:82-91

PROEFSCHRIFT

Dr. T. Buckle

17 oktober 2012
Universiteit Leiden

Promotores:
Prof. dr. J.L. Bloem
Prof. dr. C.J.H. van de Velde

Co-promotor:
Dr. F.W.B. van Leeuwen

Interventional molecular imaging, a hybrid approach

Specific detection of tumour tissue is a key feature in the diagnosis of cancer and surgery is one of the major pillars in further management of the disease.
Accurate preoperative identification, surgical planning and intraoperative visualisation can be integrated with hybrid imaging agents that contain both a radio- and fluorescent label. In this thesis both the preclinical validation and clinical introduction of this hybrid interventional molecular imaging concept is described.

Hybrid guidance for sentinel lymph node (SLN) biopsy

Hybrid nanoparticles can be used to extend SLN biopsy procedures aimed at the detection of (early) metastatic disease. A good example is the hybrid radiocolloid ICG-^{99m}Tc-nanocolloid, which is formed after mixing the clinically applied components ^{99m}Tc-nanocolloid and the fluorescent dye indocyanine green (ICG).

Preclinically, the drainage and retention pattern of ^{99m}Tc-nanocolloid and ICG-^{99m}Tc-nanocolloid were shown to be identical, while non-colloidal ICG-^{99m}Tc-human serum albumin and 'free' ICG were rapidly cleared. The drainage pattern of ICG-^{99m}Tc-nanocolloid was validated in 25 patients with melanoma or penile carcinoma. Here the hybrid approach enabled both accurate surgical planning (lymphoscintigraphy and SPECT/CT) and intraoperative detection (fluorescence), based on a single injection.

The added value of ICG-^{99m}Tc-nanocolloid during laparoscopic procedures was further shown in patients undergoing robot assisted laparoscopic prostatectomy and lymph node dissection (figure 1). During surgery, fluorescence imaging particularly improved guidance in areas with a high radioactive background signal e.g. the injection site, whereas radio-guidance was found to supplement the limited tissue penetration of the fluorescence signal. Ex vivo fluorescence imaging revealed the location of ICG-^{99m}Tc-nanocolloid injection deposits in embedded prostate samples. This enabled a direct correlation between tracer deposition and drainage pattern.

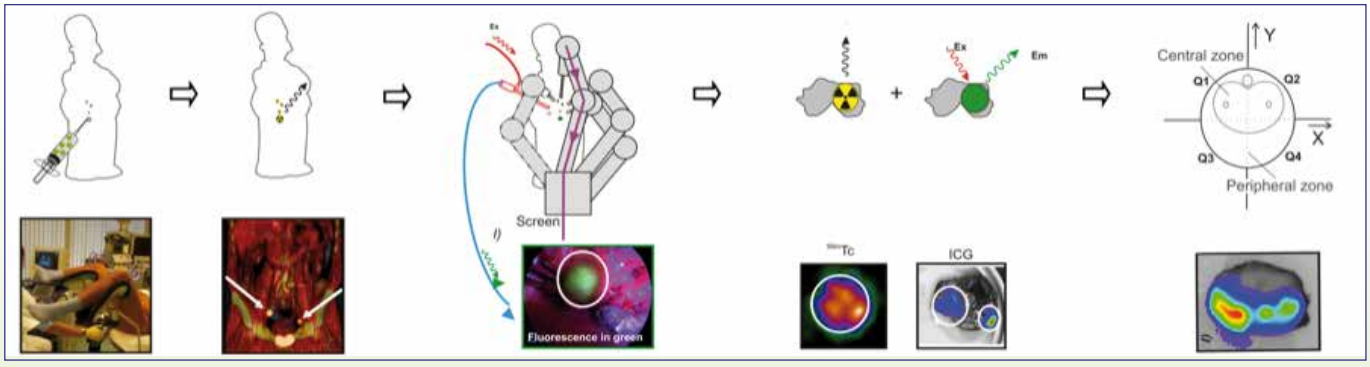

Figure 1. ***Hybrid surgical guidance during sentinel lymph node (SLN) biopsy of the prostate****. After injection of ICG-^{99m}Tc-nanocolloid preoperative lymphoscintigraphy and SPECT/CT were performed to identify the SLN. SLN biopsy was performed using a combination of radioguidance and fluorescence guidance. The radioactive and fluorescence signal in the excised SLNs was measured using a portable gamma camera and a fluorescence camera respectively. Tracer distribution was visualised in paraffin-embedded prostate samples. Distribution of fluorescence in the prostate was correlated to the number and location of the preoperatively identified SLNs.*

(Hybrid) guidance in chemokine receptor 4 (CXCR4) targeting applications

For specific visualisation of tumour cells, imaging agents that target a biomarker expressed on a tumour cell are of value. The biomarker CXCR4 is overexpressed in many types of cancer and is an emerging target in the field of molecular imaging and therapeutics.

CXCR4 targeting Ac-TZ14011 peptide derivatives are suitable for in vitro and in vivo applications. Functionalisation of Ac-TZ14011 with the fluorescent dye FITC enabled evaluation of CXCR4 expression levels and receptor localisation in vitro. ^{111}In-DTPA-Ac-TZ14011 was used to longitudinally evaluate CXCR4 expression levels in vivo, in a MIN-O mouse tumour model resembling human DCIS. Addition of a hybrid label containing a DTPA chelate and a fluorescent dye resulted in peptide with an affinity similar to that found after functionalisation with either the FITC or DTPA label. Uniquely, the hybrid derivative allowed visualisation of CXCR4 in both a pre- and intraoperative setting.

The hybrid derivative of Ac-TZ14011 also enabled integration of biomarker screening, in vivo and ex vivo validation of tumour tissue using a single agent. Flow cytometric analysis of fresh tissue biopsy specimens revealed different CXCR4 positive populations expression patterns were found to be predictive for tumour visualisation using SPECT/CT and fluorescence imaging.

Future perspectives

Further efforts were focused on fine-tuning of the utility of the hybrid surgical guidance concept. The biomarker specific hybrid approach was easily expanded to other biomarkers e.g. $\alpha_v\beta_3$ integrin. ^{111}In-MSAP-RGD, which could be used to visualise tumour margins and metastases. Alternatively, the hybrid approach was applied in combination with marker seeds and surgical navigation technologies.

Conclusions

The results described in this thesis demonstrate the potential of hybrid imaging agents in the translation of nuclear medicine findings to the operating room. The hybrid concept was shown to be of clinical value during clinical SLN biopsy procedures and during the visualisation of tumour cells in a preclinical setting. Current expansions of this exciting research field are expected to further increase the applicability of the hybrid surgical guidance concept, which will hopefully lead to patient benefit.

Additional information

Digital link to thesis available at:
www.interventionalmolecularimaging.com

Dr. E.M. van de Giessen

14 november 2012
Academisch Medisch Centrum, Universiteit van Amsterdam

Promotores:
Prof. dr. J. Booij
Prof. dr. W. van den Brink

Co-promotor:
Prof. dr. F. Baas
Dr. S.E. la Fleur

Neurobiological aspects of obesity: dopamine, serotonin, and imaging

Background

Food intake is regulated by a homeostatic system involving peripheral metabolic signals, and by a central system of cognitive, emotional, and reward-related signals in the brain. The neurotransmitters dopamine and serotonin are important in the central regulation of food intake and dysfunction of these systems might therefore be involved in the pathophysiology of overeating and obesity. Obesity has been compared to addiction, for example obese people show increased craving for food and probably have impaired inhibition like subjects with substance abuse. The aim of this thesis was to investigate the dopaminergic and serotonergic systems and brain function related to craving and inhibition.

Methods

The main focus of this thesis was the dopaminergic reward system in the striatum of the brain. Using single photon emission computed tomography (SPECT), we measured the concentration of dopamine $D_{2/3}$ receptors (^{123}I-IBZM), dopamine transporters (^{123}I-FP-CIT) and dopamine release (displacement of ^{123}I-IBZM by dexamphetamine) in obese humans. We also investigated the effects of different types of diets and anti-obesity medication on dopamine $D_{2/3}$ receptor binding (^{123}I-IBZM) in diet-induced obese rats.
Furthermore, we examined the relation between body mass index (BMI) and dopamine and serotonin transporter availability with SPECT and ^{123}I-FP-CIT.
Apart from SPECT imaging, we used functional magnetic resonance imaging (fMRI) to measure brain activation in obese and normal-weight subjects while they performed inhibition-related tasks in a MRI scanner.

Results

The most important finding was that dopamine $D_{2/3}$ receptor availability is lower in obese subjects compared to normal-weight control subjects. However, dopamine transporter availability was not different in obese subjects and neither was dopamine release induced by dexamphetamine.
This indicates that there is an imbalance in the dopamine system in the striatum in obese subjects. The lower signal transduction capacity due to lower dopamine $D_{2/3}$ receptor availability might result in a decreased reward signal (from food) in obese subjects, which subsequently could lead to compensatory overeating.
Our animal studies showed that the lower dopamine $D_{2/3}$ receptor availability in obesity is possibly induced by diets that have a high saturated fat/low carbohydrate ratio.
With respect to the serotonin system, we found higher serotonin transporter availability at subjects with high BMI, although this result is still preliminary.
Furthermore, our fMRI study showed that obese subjects did not differ from normal-weight controls in behavioural measures of inhibition, nor in brain activation. A subgroup of obese subjects with eating binges however did have impaired inhibition and reduced brain activation in de dorsolateral prefrontal cortex, a brain region involved in control.

Conclusion & future directions

This thesis shows that there are differences in the dopaminergic and serotonergic system in obesity, which are likely to play a role in the pathophysiology of the disorder. The exact relation between the striatal dopaminergic system or serotonergic system and food intake are not yet elucidated though and it will also be interesting to study the relationship with peripheral metabolic parameters.
Furthermore, we found that obese subjects in general do not show prefrontal cortex function deficits related to inhibitory control. The obese subjects with eating binges seem to form a subgroup though that has impaired inhibition and might be more closely related to addiction in behaviour and neurobiology.
Future research on the role of the brain in obesity should also focus on other neurotransmitter systems. For example, radioligands are available for the cannabinoid type 1 receptor and the μ-opioid receptor, which have both been implied in food intake regulation.

Dr. M.E. Campian

17 december 2012
Academisch Medisch Centrum, Universiteit van Amsterdam

Promotores:
Prof. dr. ir. J.M.T. de Bakker
Prof. dr. M.C. Michel

Co-promotores:
Dr. H.L. Tan
Dr. H.J. Verberne

Pathophysiology of right ventricular heart disease: The role of structure, apoptosis and inflammation

Heart failure, a major and still growing public health problem, appears to result not only from cardiac overload or injury but also from a complex interplay among genetic, neurohormonal, inflammatory, and biochemical changes acting on cardiomyocytes, the cardiac interstitium, or both. Multitudes of recent studies suggest that loss of terminally differentiated cardiac myocytes contributes to the development of heart failure. Studies have reported that apoptosis occurs in myocardial tissue samples from patients suffering from myocardial infarction, dilated cardiomyopathy and end-stage heart failure (1-4) as well as in animal models of ischemia-reperfusion injury (5-7). Apoptosis is activated in cardiomyocytes by multiple stressors that are commonly seen in cardiovascular disease such as cytokine production (8, 9), increased oxidative stress (10), and DNA damage (11).

It is generally accepted that apoptosis plays an important role in left ventricular (LV) disease (12). While initial studies of LV failure reported unrealistically high levels of apoptotic cell death (13), later work has consistently shown that approximately 80-250 cardiomyocytes per 10^5 cardiac nuclei undergo apoptosis at any given time in patients with late-stage dilated cardiomyopathy (14-16). In contrast, the base-line rate of apoptosis in healthy human hearts is only 1-10 cardiomyocytes per 10^5 nuclei. Whether the chronically elevated but extremely low level of apototic cardiomyocytes observed in LV failing hearts plays a causal role remains a controversial issue with major therapeutic implications. In contrast, the association of apoptosis with right ventricular (RV) disease progression is unclear (17, 18).

The monocrotaline (MCT) rat model is commonly used as a model of pulmonary hypertension that leads to RV hypertrophy and RV failure. Using this MCT rat model we demonstrated that apoptosis exhibits a particular time course, peaking at early disease stages (RV hypertrophy) and declining thereafter (RV failure), but remaining significantly increased over baseline values at all RV disease stages. Furthermore, we showed that serial technetium-99m annexine (^{99m}Tc-ANX V) scintigraphy can be used to monitor apoptosis throughout RV disease progression in a noninvasive manner. ^{99m}Tc-ANX V binds to exposed phosphatidylserine on the outer surface of apoptotic cells (20), this allows for the visualisation and localisation of apoptotic cells. Also, we found that a delay in RV disease progression by an angiotensin II receptor antagonist (i.e. valsartan) was attended by a reduction in RV apoptosis (19).

This observation not only illustrates that serial *in vivo* ^{99m}Tc-ANX V scintigraphy may be used to monitor the effects of therapy aimed at counteracting apoptosis, but supports the notion that apoptosis is causally related to RV disease. Still, it must be noted that it does not prove a causal relation, because RV disease progression was not completely arrested and apoptosis was not completely abolished. The reported percentage of apoptosis in end-stage LV failure is similar to our findings in the RV failure stage (14). The occurrence of apoptosis during early RV disease stages suggests a potentially beneficial effect of apoptosis inhibition. Studies from a transgenic mouse model of cardiac-restricted expression of ligand-activated pro-caspase 8 have demonstrated that even low levels of cardiomyocyte apoptosis are sufficient to cause lethal dilated cardiomyopathy. Most significantly, the treatment with caspase inhibitors prevents cardiac dilatation and attenuates cardiac decomposition (21).

Since the regenerative capacity of the myocardium is limited, there is a strong interest in the prevention of cardiomyocyte loss in cardiovascular diseases to prevent development of heart failure.

Apart from apoptosis, the past decade has provided increasing evidence that inflammation is involved in the clinical deterioration of patients with LV failure, with increased production and enhanced release of pro-inflammatory

cytokines. Patients with heart failure have high plasma levels of tumor necrosis factor-alpha (TNF-α), and soluble TNF-α receptors 1 and 2 serve as prognostic markers in this population (22).

The association between immune-inflammatory activation and RV disease progression is an essential observation in our study. The inflammatory activation exhibited a particular time course, becoming elevated at an early disease stage (RV hypertrophy), peaking at the stage of RV dilation, and remaining elevated compared to baseline throughout disease progression to RV failure. Furthermore, the immune-inflammatory response was non-invasively assessed with gallium-67 (^{67}Ga) scintigraphy and reflected local inflammation in RV, as confirmed by ^{67}Ga autoradiography, immunohistochemistry, and gene expression profiles (23).

Over the last years, two large clinical studies were conducted with TNF-α blockers in patients with LV failure. The RENAISSANCE study used Etanarcept and the ATTACH study used Infliximab (24). Both agents directly antagonised TNF-α but did not prove to have any clinical benefit (25). One possible explanation for the lack of response to Etanarcept is that it is a highly selective TNF-α inhibitor, and this compound has no cross-reaction with any known cytokine, and the highly selective nature of this compound could be a disadvantage (22, 25). One other argument is that the immune system is redundant and other pro-inflammatory cytokines (interleukin 1-beta, interleukin 6, and transforming growth factor-beta) can participate in the process of heart failure. Following this concept, there are now at least two forms of non-specific immunomodulatory strategies under investigation: the intravenous gamma globulin (26, 27) and immunoadsorption (28).

A better understanding of the mechanism of RV failure may enable us to find a better cure and improve the prognosis. Will it be a better insight into the apoptotic cascade or the inflammatory system? Will it be the ability to manipulate the immunological system or maybe stem cell transplantation? Which one of these approaches will open the door to long-term success in the fight against RV failure? This enigma has yet to be solved.

The remodeling of the RV myocardium in rare diseases such as arrhythmogenic right ventricular cardiomyopathy/dysplasia (ARVC/D) and the Brugada syndrome (BrS) was further focus of our investigation.

Regardless of the mode of inheritance, it appears that the majority of ARVC/D-related genes encode for proteins that make up desmosomes, which are intracellular adhesion complexes that provide mechanical connections between cardiac myocytes. When placed under mechanical stress, the impaired desmosomes cause myocytes to detach from each other leading to cell death (29, 30). This cell death causes inflammation with scar formation and fat deposition.

Since ARVC/D involves focal areas of the RV and spares the inter-ventricular septum, myocardial biopsy tends to have a low sensitivity and specificity. Myocardial biopsy of the RV free wall may increase the diagnostic yield, at the risk of increased perforation rate. Moreover, some degree of fat is interspersed between myocytes in healthy individuals, affecting the specificity of the biopsy sample. Conversely, in early stages of ARVC/D changes to the myocardium may not be well developed and not be detected in the biopsy.

In ARVC/D, we conducted studies using ^{99m}Tc-ANX V and ^{67}Ga-scintigraphy. Our results demonstrate increased ^{99m}Tc-ANX V uptake in the RV free wall of ARVC/D patients, suggestive of RV-specific apoptotic activity in these patients (31). Also, with a combined analysis of plasma level of inflammatory cytokines and cardiac ^{67}Ga-scintigraphy, we demonstrate that myocardial inflammation can be noninvasively detected in ARVC/D patients (32). *In vivo* imaging approaches play an important role in understanding the complex pathophysiological mechanisms underlying ARVC/D disease progression, thus aiding in the development of tailored and efficient therapeutic tools.

The cardiac sodium channel controls cardiac excitability. The $Na_v1.5$ is a sodium ion channel protein that in humans is encoded by the *SCN5A* gene. *SCN5A* mutations that result in loss-of-function of $Na_v1.5$ are associated with various inherited arrhythmia syndromes that revolve around reduced cardiac excitability (i.e. "loss-of-function *SCN5A* channelopathy"). The Brugada syndrome (BrS) is the best know example of such a loss-of-function *SCN5A* channelopathy. It has long been assumed that cardiac structural abnormalities are undetectable by standard clinical imaging methods in individuals with loss-of-function *SCN5A* channelopathies. We found evidence that patients with BrS had enlargement of both RV and LV, as measured by cardiac magnetic resonance imaging (33). These results support the idea that $Na_v1.5$ is not only pivotal in control of cardiac excitability but is also involved in maintaining structural integrity of the heart.

The increasing recognition of the importance of RV dysfunction in the pathogenesis and outcomes of many cardiovascular diseases have led to resurgence in interest in assessing its pathological remodeling and function. While many challenges remain, the last decades have yielded improved knowledge on the understanding of the pathophysiological mechanisms underlying RV failure progression.

References

1. Olivetti G, Quaini F, Sala R, et al. Acute myocardial infarction in humans is associated with activation of programmed myocyte cell death in the surviving portion of the heart. J Mol Cell Cardiol. 1996;28:2005-16
2. Saraste A, Pulkki K, Kallajoki M, et al. Apoptosis in human acute myocardial infarction. Circulation. 1997;95:320-3
3. Narula J, Haider N, Virmani R, et al. Apoptosis in myocytes in end-stage heart failure. N Engl J Med. 1996;335:1182-9
4. Aharinejad S, Andrukhova O, Lucas T, et al. Programmed cell death in idiopathic dilated cardiomyopathy is mediated by suppression of the apoptosis inhibitor Apollon. Ann Thorac Surg. 2008;86:109-14
5. Cheng W, Kajstura J, Nitahara JA, et al. Programmed myocyte cell death affects the viable myocardium after infarction in rats. Exp Cell Res. 1996;226:316-27
6. Gottlieb RA, Burleson KO, Kloner RA, Babior BM, Engler RL. Reperfusion injury induces apoptosis in rabbit cardiomyocytes. J Clin Invest. 1994;94:1621-8
7. Gao HK, Yin Z, Zhou N, et al. Glycogen synthase kinase 3 inhibition protects the heart from acute ischemia–reperfusion injury via inhibition of inflammation and apoptosis. J Cardiovasc Pharmacol. 2008;52:286-92
8. Kubota T, McTiernan CF, Frye CS, et al. Dilated cardiomyopathy in transgenic mice with cardiac-specific overexpression of tumor necrosis factor-alpha. Circ Res. 1997;81:627-35
9. Bryant D, Becker L, Richardson J, et al. Cardiac failure in transgenic mice with myocardial expression of tumor necrosis factor-alpha. Circulation. 1998;97:1375-81
10. Sayen MR, Gustafsson AB, Sussman MA, Molkentin JD, Gottlieb RA. Calcineurin transgenic mice have mitochondrial dysfunction and elevated superoxide production. Am J Physiol Cell Physiol. 2003;284:C562-70
11. Wang J, Silva JP, Gustafsson CM, Rustin P, Larsson NG. Increased in vivo apoptosis in cells lacking mitochondrial DNA gene expression. Proc Natl Acad Sci USA. 2001;98:4038-43
12. Anversa PL, Leri A, Beltrami CA, Guerra S, Kajstura J. Myocyte death and growth in the failing heart. Lab Invest. 1998;78:767-86
13. Narula J, Haider N, Virmani R, et al. Apoptosis in myocytes in end-stage heart failure. N Engl J Med. 1996;335:1182-9
14. Olivetti G, Abbi R, Quaini F, et al. Apoptosis in the failing human heart. N Engl J Med. 1997;336:1131-41
15. Saraste A, Pulkki K, Kallajoki M, et al. Cardiomyocyte apoptosis and progression of heart failure to transplantation. Eur J Clin Invest. 1999;29:380-6
16. Guerra S, Leri A, Wang X, et al. Myocyte death in the failing human heart is gender dependent. Circ Res. 1999;85:856-66
17. Ecarnot-Laubriet A, Assem M, Poirson-Bichat F, et al. Stage-dependent activation of cell cycle and apoptosis mechanisms in the right ventricle by pressure overload. Biochim Biophys Acta. 2002;1586:233-42
18. Ikeda S, Hamada M, Hiwada K. Cardiomyocyte apoptosis with enhanced expression of P53 and Bax in right ventricle after pulmonary arterial banding. Life Sci. 1999;65:925-33
19. Campian ME, Verberne HJ, Hardziyenka M, et al. Serial noninvasive assessment of apoptosis during right ventricular disease progression in rats. J Nucl Med. 2009;50:1371-7
20. Blankenberg FG, Katsikis PD, Tait JF, et al. In vivo detection and imaging of phosphatidylserine expression during programmed cell death. PNAS. 1998;95:6349-54
21. Wencker D, Chandra M, Nguyen K, et al. A mechanistic role for cardiac myocyte apoptosis in heart failure. J Clin Invest. 2003;111:1497-504
22. Mann DL. Recent insights into the role of tumor necrosis factor in the failing heart. Heart Fail Rev. 2001;6:71-80
23. Campian ME, Hardziyenka M, de Bruin K, et al. Early inflammatory response during the development of right ventricular heart failure in a rat model. Eur J Heart Fail. 2010;12:653-8
24. Anker SD, von Haehling S. Inflammatory mediators in chronic heart failure: an overview. Heart. 2004; 90:464-70
25. von Haehling S, Jankowska EA, Anker SD. Tumor necrosis factor alpha and the failing heart-pathophsiology and therapeutic implication. Basc Res Cardiol. 2004;99:8-28
26. McNamara DM, Holubkov R, Starling RC, et al. Controlled trial of intravenous immune globulin in recent onset dilated cardiomyopathy. Circulation. 2001;103:2254-9
27. Gullestad L, Aass H, Fjeld JL, et al. Immunomodulation therapy with intravenous immunoglobulin in patients with chronic heart failure. Circulation. 2001;103:220-5
28. Muller J, Wallukat G, Dandel M, et al. Immunoglobulin adsorption in patients with idiopathic dilated cardiomyopathy. Circulation. 2000;102:385-91
29. Sen-Chowdhry S, Lowe MD, Sporton SC, McKenna WJ. Arrhythmogenic right ventricular cardiomyopathy: clinical presentation, diagnosis, and management. Am J Med. 2004;117:685-95
30. Sen-Chowdhry S, Syrris P, McKenna WJ. Genetics of right ventricular cardiomyopathy. J Cardiovasc Electrophysiol. 2005;16:927-35
31. Campian ME, Tan HL, van Moekerken AF, Tukkie R, et al. Imaging of programmed cell death in arrhythmogenic right ventricle cardiomyopathy/dysplasia. Eur J Nucl Med Mol Imaging. 2011;38:1500-6
32. Campian ME, Verberne HJ, Hardziyenka M, et al. Assessment of inflammation in patients with arrhythmogenic right ventricular cardiomyopathy/dysplasia. Eur J Nucl Med Mol Imaging. 2010; 7:2079-85
33. van Hoorn F, Campian ME, van der Wal A, et al. The cardiac sodium channel is involved in maintaining structural integrity of the heart. PLoS One. 2012;7:e42037

PROEFSCHRIFT

Dr. M. Brom

15 januari 2013
Radboud Universiteit
Nijmegen

Promotores:
Prof. dr. M. Gotthardt
Prof. dr. O.C. Boerman

Development of a tracer to image pancreatic beta cells

Beta cells are the insulin-producing cells in the islets of Langerhans of the pancreas. Beta cell mass (BCM) plays an important role in the pathogenesis of both type 1 and type 2 diabetes. However, due to the lack of a non-invasive method to determine the BCM, changes in BCM and the relation with beta cell function are still unknown. The aim of the studies described in this thesis was to develop and characterise a tracer to determine the BCM *in vivo*. An ideal tracer for the determination of the BCM should have high and specific uptake in the beta cells and low uptake in the exocrine and other endocrine cells. Moreover, low uptake in surrounding non-target tissues is required, for a good target-to-background ratio. Furthermore, the uptake of the tracer should correlate with the BCM and the difference in uptake between healthy and diabetic individuals has to be large to enable detection of small differences in BCM. The tracer used in the studies described in this thesis is radiolabelled exendin that binds to the glucagon-like peptide-1 receptor (GLP-1R) specifically expressed on the beta cells.

In the first chapters the labelling of exendin with indium-111 (^{111}In) and gallium-68 (^{68}Ga) and subsequent purification was optimised. After optimisation of the labelling the in vitro and in vivo targeting characteristics of ^{68}Ga- and ^{111}In-labelled exendin were examined using competitive binding and internalisation assay using GLP-1R expressing INS-1 (insulinoma) tumour cells. In addition, biodistribution and imaging studies were performed in BALB/c nude mice with subcutaneous INS-1 tumours. From these studies, the optimal peptide for beta cell targeting was selected: ^{111}In-exendin.
Then the ability to determine the beta cell mass with exendin was examined by single photon emission computed tomography (SPECT) imaging after injection of ^{111}In-exendin in a rat model for acute beta cell loss. Biodistribution studies in Brown Norway rats showed GLP-1R-mediated uptake in the pancreas. Chemical destruction of the beta cells by alloxan resulted in a pancreatic uptake that was >80% lower than in control rats. These results indicated beta cell specific uptake of ^{111}In-labelled exendin. These results were confirmed by autoradiography: digital autoradiography showed various hot spots throughout the pancreas, representing the islets of Langerhans, with low uptake in the exocrine pancreas. The hot spots observed with digital autoradiography colocalised with the expression of insulin as determined immunohistochemically, indicating that the hotspots were indeed the insulin-producing beta cells. Gradual destruction of the beta cells by injecting various doses of alloxan resulted in reduction of the intensity of the hot spots; the number of hot spots was massively decreased in severely diabetic rats. Microautoradiography showed specific localisation of ^{111}In-labelled exendin in the islets of Langerhans that colocalised with insulin staining. Moreover, the uptake of ^{111}In-exendin measured by ex vivo counting correlated with the BCM as determined by morphometric analysis. The pancreas could be visualised in healthy rats and the signal was almost absent in severely diabetic rats. Most importantly, the uptake could be quantified in the SPECT images and the uptake correlated linearly with the beta cell mass, as determined by morphometric analysis.
In conclusion, ^{111}In-exendin is a promising tracer for the non-invasive determination of the BCM.

Cursus IDKD musculoskeletaal in Davos

Inschrijfkosten:	gehele cursus ± 1000 euro NM Diamond Course ± 400 euro
aantal deelnemers:	gehele cursus ± 800 personen NM Diamond Course ± 90 personen
accreditatiepunten:	gehele cursus 24 punten NM Diamond Course 8 punten
website en registratie:	www.idkd.org

Als je radiologen vraagt naar een goede cursus beginnen ze unaniem over de IDKD cursus in Davos. Deze Zwitserse club is erin geslaagd om elk voorjaar een hands-on training te organiseren met sprekers van wereldformaat. In een cyclus van vier jaar komen verschillende thema's aan bod. Ik was vooral geïnteresseerd in musculoskeletaal (MSK) vanwege onze grote toename in SPECT/CT verrichtingen bij de orthopedie. Vooral nascholing op CT gebied leek me nuttig, zeker nu onze CT van een prachtige diagnostische kwaliteit is. Daarbij wilde ik namens de onderwijscommissie graag eens zien hoe de top van radiologisch onderwijs eruitziet, dus ik schreef me direct in voor de hele week.

In Davos bleek ik niet de enige Nederlandse nucleair geneeskundige te zijn met dit idee, meerdere collega's waren het hooggebergte ingetrokken. Ook de Nederlandse radiologen waren goed vertegenwoordigd. En voor degenen die denken dat Davos wel vooral skiën zal zijn, met naast après-ski een beetje cursus: dat was dit jaar helaas in het geheel niet het geval, de dagen waren van 9 tot 5 volgepland. Gelukkig liep de après-ski wat uit en was het ook 's avonds nog gezellig.

Heel praktisch begon de cursus met een Diamond Course nucleaire met op de tweede dag nog een ochtend nucleaire. De rest van de week bestond uit radiologie, met vooral heel erg veel MRI. Het nucleaire deel was zeer nuttig, er waren goede sprekers met relevante verhalen.
Het is werkelijk hands-on, heel modern en praktisch met een BYOD opzet (bring your own device, = laptop).
We kregen een USB-stick vol casuïstiek in een overzichtelijk programma, en zo zat een zaal vol ijverige dokters te puzzelen en te scrollen. Niet echt 3D SPECT, vooral planaire series.
De zalen waren prettig klein, met niet meer dan dertig man, dus er was genoeg mogelijkheid tot interactief lesgeven. Nu was niet elke spreker even behendig in deze interactie, maar de meesten kregen goed contact met de cursisten, en er was volop discussie. Er was veel interessante casuïstiek, met uitgebreide achtergrondinformatie. Zo blijkt dat in Zwitserland 'cost not an issue' is voor PET, en worden in Tel Aviv ^{18}F-PET scans gemaakt vanwege de lage stralingsdosis.
Een aanrader dus, deze Diamond Course, als update voor nucleair geneeskundigen met MSK ervaring, of voor beginnende specialisten. Een paar dagen focussen op één vakgebied werkt erg goed.

De overige dagen bestonden uit heel veel MRI, en waren voor een nucleair geneeskundige minder relevant. CT wordt maar weinig gebruikt voor MSK. De zojuist als hoogleraar aangestelde MSK specialist uit het AMC, Mario Maas, gaf een schoolvoorbeeld van modern lesgeven door een groot deel van de zaal aan het woord te laten, en uitgebreid in te gaan op gesuggereerde diagnoses. Dat geeft een enorme betrokkenheid bij de toch vaak lastige onderwerpen.

Klein minpuntje was de vaste indeling in groepen. Officieel mocht je niet aansluiten bij een spreker die jouw voorkeur heeft, dit in verband met de zaalgrootte. De soms erg volle zalen gaven het vermoeden dat veel specialisten, eigenwijs als ze zijn, toch voor de beste sprekers waren gegaan. Ander minpuntje is de forse prijs en de relatief lange reis. Dat laatste is echter heel goed op te lossen als je de cursus combineert met wat dagen in de sneeuw.

Ik denk dat Davos terecht een naam heeft als top in nascholing beeldvormende techniek. De NVNG kan hier veel van leren, en ik hoop die lessen ook mee te kunnen nemen in onze komende nascholingsprogramma's, in ieder geval in onze komende nascholing MSK dit najaar in Arnhem.

Dr. J. Lavalaye
nucleair geneeskundige Sint Antonius ziekenhuis Nieuwegein
voorzitter onderwijscommissie NVNG

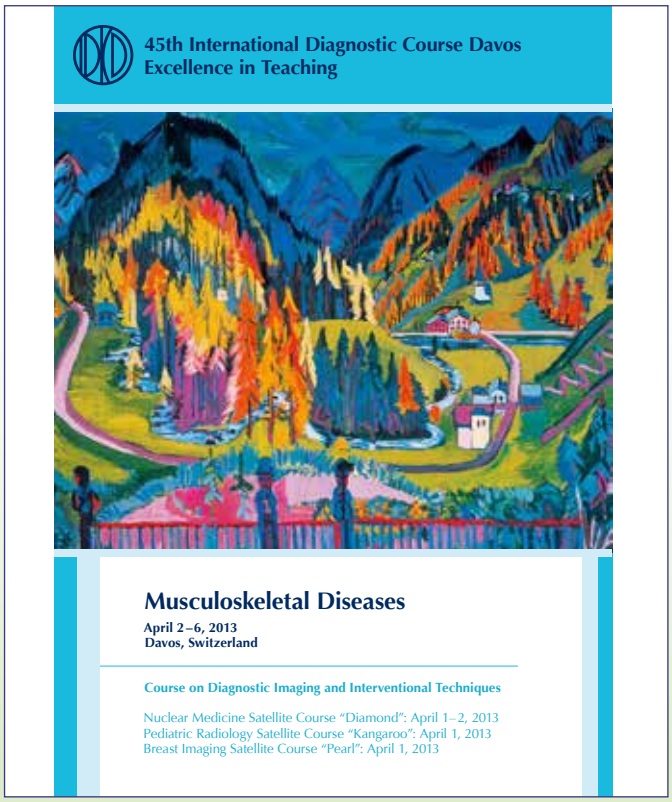

AIOS-cursus Radiofarmacie

Op donderdag 8 november 2012 werd door de NvNG onderwijscommissie de cursus Radiofarmacie georganiseerd in het UMC St. Radboud te Nijmegen. Gastheer en gastvrouw waren dr. H.H. Boersma (ziekenhuisapotheker UMC Groningen) en mevr. dr. L. Prompers (nucleair geneeskundige Academisch Ziekenhuis Maastricht).

inschrijfkosten:	120 euro aspirant-leden 145 euro leden 185 euro niet-leden
aantal deelnemers:	79
registratie:	bureau NvNG
accreditatiepunten:	6
website:	www.nvng.nl / www.umcn.nl

Na 's ochtends wakker te zijn geschrokken van een enorme explosie, die naar later bleek bij de plaatselijke energiecentrale had plaatsgevonden, togen wij naar een fraaie binnentuin in het nieuwe gedeelte van het UMC St. Radboud.
Het spits werd afgebeten door professor Boerman met een enthousiast verhaal over de werking van de (molybdeen) generator, de labeling met onderliggende radiochemie van met name technetiumpreparaten en de kwaliteitscontroles die hierbij komen kijken.
Gedurende de dag werd verder gesproken over de ontwikkeling van nieuwe radiofarmaca -from bench to bedside- en over farmacodynamiek van veelgebruikte radiofarmaca. Uiteraard kwam de regelgeving rondom het bereiden van radiofarmaca/GMP aan bod, en waren er voorbeelden van praktische zaken die van belang zijn bij het verkrijgen van een GMP-z approval. Ook werd aandacht geschonken aan productietechnieken van verschillende isotopen en de achterliggende fundamentele principes.
Bij dit brede scala aan onderwerpen zijn vanzelfsprekend sprekers vanuit vele disciplines (radiochemici, klinisch fysici, apothekers, nucleair geneeskundigen) aan het woord gekomen, afkomstig uit het gehele land. Zo werd het een leerzame dag met een even divers docenten- als toehoorderspalet, een gevarieerd vakgebied als de Nucleaire Geneeskunde waardig.

drs. B. Bulten
drs. R. Hermsen
AIOS Nucleaire Geneeskunde
UMC St. Radboud, Nijmegen

Second Tübingen PET/MR Workshop 2013

organisatie:	Eberhard Karis Universität Tübingen
website:	www.pet-mr-tuebingen.de
datum:	8-12 april 2013
inschrijfkosten:	1150 – 1350 euro voor nucleair geneeskundigen 800-1000 euro voor AIOS
aantal deelnemers:	80
specialismen:	nucleair geneeskundigen, radiologen, klinisch fysici
accreditatie NVNG:	24 accreditatiepunten
cursusmateriaal:	handboek met hand-outs van presentaties (niet allemaal)

Het doel van deze cursus wordt door de organisatie als volgt beschreven:

- het geven van een platform voor het uitwisselen van ervaringen en ideeën tussen afgevaardigden vanuit de beeldvormende technieken en klinische disciplines, inclusief collega's met uitgebreide ervaring in PET/MRI;
- zorgen voor het uitwisselen van ideeën, twijfels en mogelijkheden van de gecombineerde PET/MRI in diagnostische flow-charts en de researchmogelijkheden binnen de geneeskunde.

Programma
De cursus was verdeeld over vijf dagen. Elke dag werd gestart met een gezamenlijke sessie (grand rounds), gevolgd door meerdere gelijktijdige sessies (tutorials, dialogue boards en hands-on's). De indeling voor deze sessies was gebaseerd op de voorkeuren die de deelnemer voorafgaand aan de cursus kon opgeven. Twee dagen werden afgesloten met een round-table discussie. Eén middag werd besteed aan presentaties vanuit de industrie. Een korte samenvatting van de verschillende sessies:

- *grand rounds*
  presentaties gegeven door een expert met een grote variatie aan onderwerpen, gerelateerd aan de PET/MRI (stand van zaken PET/MRI, geavanceerde PET/MRI

applicaties, veiligheidsaspecten, preklinische toepassingen van PET/MRI), maar ook aan gebieden buiten de PET/MRI (de toekomst van PET/CT en PET tracer ontwikkelingen);
- *tutorials*
  presentaties gegeven voor kleinere interactieve groepen deelnemers, over de basisaspecten en geavanceerde mogelijkheden van PET, PET/CT, MRI en PET/MRI;
- *dialogue boards*
  aantal kortere presentaties waarin de eerste klinische en wetenschappelijke ervaringen met PET/MRI verteld werden (oncologie, neurologie, kinderoncologie, kwantificatiemethoden, standaardisatie en workflows);
- *hands-on's*
  bezoek aan een MRI, PET/CT of PET/MRI camera, waarin voorbeelden van de dagelijkse praktijk werden gegeven en casuïstiek werd besproken;
- *round-table discussies*
  gezamenlijke interactieve sessies over reïmbursement van de PET/MRI en discussie over de killer applicatie van de PET/MRI.

Evaluatie

De workshop werd gehouden in een inspirerende omgeving. Tübingen is een vriendelijk, gezellig stadje en de universiteit en kliniek zijn uniek gelegen op de Schnarrenberg, uitkijkend over het oude stadscentrum. De accommodaties waren prima geregeld en de catering uitstekend verzorgd. De organisatie van de workshop was ook zeer benaderbaar, leidend tot een uitstekende interactie met de deelnemers. Over het algemeen werden de presentaties en tutorials gegeven door key onderzoekers en key opinion leaders hoewel die meestal Duits getint waren en hand-outs niet altijd overeenkwamen met de slides die werden gepresenteerd. Hierdoor was het geheel soms wat moeilijk volgen. Hoogtepunt van de cursus waren de presentaties van professor Sabri (Leipzig) die duidelijk zijn zeer vooruitstrevende mening over de unieke mogelijkheden van de PET/MRI naar voren bracht en van professor Czernin (Los Angeles), die duidelijk meer twijfels had over de meerwaarde van PET/MRI ten opzichte van de PET/CT. Dit leverde boeiende discussies op tussen beide heren en de deelnemers van de workshop. Er werd ook veel gediscussieerd over wat nu de 'killer applicatie' (dé klinische toepassing van de PET/MRI) was en of de PET/MRI zonder deze 'killer applicatie' wel levensvatbaar zou zijn. Op dit moment echter bestaat die 'killer applicatie' helaas niet. Natuurlijk zijn er gebieden waarin de PET/MRI meerwaarde kan hebben (neurologie, cardiologie, gynaecologische tumoren, neuro-endocriene tumoren, borstkanker, prostaatkanker, kinderoncologie), maar dé meerwaarde boven PET/CT is op dit moment nog niet geheel duidelijk. Vanuit klinisch-fysisch standpunt was de discussie over de acceptatietests van een hybride PET/MRI systeem interessant; hieruit bleek dat toch speciaal aandacht dient te worden besteed aan invloed van de verschillende coils op de attenuatiecorrectie. Daarnaast bleek ook dat uitdagingen op het vlak van kwantificatie en attenuatiecorrectie vooral betrekking hebben op het thoraxgebied.
In het algemeen werden de beschreven doelstellingen van de cursus niet gehaald. De uitwisseling tussen beeldvormers en clinici werd niet bereikt, vooral omdat er nauwelijks bijdragen van clinici waren. Duidelijke klinische flow-charts voor het gebruik van PET/MRI werden ook niet gegeven. Van een echte opbouw in de cursus was geen sprake en geregeld ontbrak ook de afstemming tussen de diverse presentaties. Het gehele programma was enigszins beperkt voor de lengte van de cursus, resulterend in lange pauzes. Ons inziens had de gehele inhoud van de cursus ook in drie dagen gekund.
Er werd geen rekening gehouden met de achtergrond van de deelnemers. Zo kon je als nucleair geneeskundige terechtkomen in een geheel fysische sessie en vice versa. De grand rounds waren te verschillend van aard, niet allemaal toegespitst op PET/MRI. Opbouw in de tutorials (basis en geavanceerd) was er ook niet altijd. Zo werden er in de geavanceerde PET/MRI tutorial voornamelijk basisaspecten besproken, terwijl in de basis PET/MRI tutorial voornamelijk preklinische camera-ontwikkelingen naar voren kwamen. Afstemming tussen de tutorials met dezelfde onderwerpen was er niet. De hands-on's vielen enigszins tegen. Waar gehoopt werd op een praktische invulling van deze sessies waarbij geleerd zou kunnen worden welke MRI sequenties belangrijk zijn voor welke indicatie, werd voornamelijk de werking van de camera getoond met af en toe wat casuïstiek. Naar ons idee is de organisatie er niet geheel in geslaagd om aan onze verwachtingen te voldoen. Wetenschappelijk en klinisch gezien viel het enigszins tegen. De deelnemers konden tijdens de cursus ook een evaluatieformulier invullen. De omgeving, accommodatie en vriendelijkheid van de organisatie maakten echter veel goed.

Conclusie

In het algemeen maakte de 2nd Tübingen PET/MR workshop haar beloftes niet geheel waar. In haar huidige vorm zullen wij de cursus niet aanbevelen aan onze collega's. Aanpassingen aan het huidige programma (meer afstemming tussen de presentaties, hands-on's meer geschikt maken voor de klinische praktijk, onderverdeling tussen sessies voor nucleair geneeskundigen en voor klinisch fysici) zullen noodzakelijk zijn om een 3e workshop (al gepland van 17 tot 21 februari 2014) tot een succes te maken. Desalniettemin hebben wij genoten van de prima atmosfeer tijdens de workshop en van Tübingen zelf.

Ronald van Rheenen, Andor Glaudemans, Riemer Slart
nucleair geneeskundigen, Universitair Medisch Centrum Groningen

Michel Koole
klinisch fysicus, Universitair Medisch Centrum Groningen

Maurits Wondergem
nucleair geneeskundige, Medisch Centrum Alkmaar

AZ Sint-Jan AV Brugge

Dr. F. De Geeter

Afdeling Nucleaire Geneeskunde, AZ Sint-Jan AV, Brugge

AZ Sint-Jan AV, Brugge

Wie de Brugse binnenstad heeft bezocht, heeft het minstens gezien, en mogelijk zelfs met een bezoek vereerd: het Brugse Sint-Janshospitaal. In oorsprong daterend uit de 12de eeuw is het een van de oudste bewaarde ziekenhuisgebouwen in Europa. Het bestaat in essentie uit drie middeleeuwse ziekenzalen, waaraan later nog een broeder- en een zusterklooster werden toegevoegd. Het is nu ingericht als museum en toont onder meer het Ursulaschrijn, een meesterwerk van de Vlaamse Primitief Hans Memling, die in de 15de eeuw in Brugge werkte en het schrijn voor het Sint-Janshospitaal vervaardigde. Ook het altaarstuk met Sint-Jan de Doper en Sint-Jan de Evangelist, de patroonheiligen van het hospitaal, is er te zien.

Op dezelfde campus werd halverwege de 19de eeuw een nieuw ziekenhuis gebouwd, een centrale gang met daarrond acht ziekenzalen. In de loop van de jaren werden tussen de zalen en rond het gebouw allerlei bijgebouwtjes toegevoegd, tot het geheel zo'n wanordelijk kluwen werd, dat men besliste te verhuizen naar de huidige campus, op een boogscheut van de binnenstad. Het negentiende-eeuwse ziekenhuis doet nu dienst als congres- en evenementencentrum. Het was ergens in de kelders van dat ziekenhuis dat de nucleaire geneeskunde in Sint-Jan een aanvang nam.
Het huidige ziekenhuis werd gebouwd in de zeventiger jaren van de vorige eeuw, in een tijdloze architectuur. Ofschoon het 'op de groei' werd bedacht, zoals we dat in Vlaanderen zeggen, dit wil zeggen voldoende ruim om uitbreidingen te kunnen accommoderen, ondergaat ook dit gebouw nu het lot van zijn voorganger. In hoog tempo worden allerlei uitbreidingen geconstrueerd, die naar de smaak van de auteur niet altijd voldoende respect hebben voor de bestaande architectuur. De dienst nucleaire geneeskunde bevindt zich te paard over zo'n uitbreiding en het oude gebouw. Bij die uitbreiding werd erover gewaakt dat de dienst voldoende licht zou binnenlaten, en dat heeft geleid tot een centrale lichtstraat, die een blik geeft op het uitspansel. Een bezoekende arts uit Nederland, bekend met talloze nucleaire diensten in Nederland en Vlaanderen, vond onze dienst architecturaal een van de meest luchtige diensten die hij had bezocht. Van 'unclear medicine' geen sprake hier: daglicht!

De oude waarden van het middeleeuwse Sint-Janshospitaal waren nog altijd rond in de moderne infrastructuur. Het gasthuis stond vroeger in de eerste plaats open voor behoeftigen en zieken. Nu formuleert de visie van het

ziekenhuis het als volgt: 'innovatieve referentiezorg voor iedereen'. Laagdrempelig dus, ook voor de sociaal zwakkeren – dat is dus niet veranderd.

Van meet af aan maakte de dienst nucleaire geneeskunde organisatorisch deel uit van het Oncologisch Centrum, dat daarnaast ook nog de afdelingen medische oncologie en radiotherapie omvat. Historisch is dat te verklaren doordat de dienst zich, zoals in vele ziekenhuizen in Vlaanderen, ontwikkelde vanuit de radiotherapie. Het eerste diensthoofd, dr. Alfons Declercq, was radiotherapeut van opleiding en beoefende daarnaast de nucleaire geneeskunde. Hij bleef lange jaren het enige staflid, tot dat op het eind van de tachtiger jaren onhoudbaar bleek. Het eerstvolgende staflid, dr. Frank De Geeter, schrijver dezes, behoorde tot de eerste lichting nucleair geneeskundigen die als dusdanig werden erkend en voor wie de bekwaming in de nucleaire geneeskunde geen aanhangsel was bij een andere specialistische erkenning. In 1999, rond de pensionering van dr. Declercq, werd de medische staf versterkt met dr. Anja Van den Eeckhaut, en in 2002 met dr. Natascha Walgraeve. Elk van de nucleair geneeskundigen heeft een wat verschillend profiel: de een al wat meer klinisch dan de ander, of wat meer theoretisch, of wat meer geïnteresseerd in de apparatuur. Dr. Van den Eeckhaut legt zich ook toe op de pediatrische nucleaire geneeskunde. Vooral dr. Van den Eeckhaut en dr. Walgraeve houden zich bezig met de metabole radiotherapie.

De dienst beschikt over een ruime en up-to-date infrastructuur. In 1989 bezat de dienst een roterende eenkopscamera (die het nog zou uitzingen tot in 2007), een rijdende eenkopscamera voor whole body opnamen (die minstens drie passages vergden, omdat het veld van de ronde detector te klein was om in één passage de volle breedte van de patiënt te scannen) en een Pho-gamma 5 (die Polaroid prentjes produceerde waarop dezelfde structuur in drie verschillende exposities werd afgebeeld). Enige jaren later werd een dubbelkopse whole body camera gekocht met rechthoekige detectoren en nog een paar jaar later een driekopscamera. Ondertussen werd de beeldvorming meer en meer digitaal en werden de foto's op röntgenfilm met natte ontwikkeling geleidelijk vervangen door droge ontwikkelingsprocedés. Vanaf 2007 werden alle beelden doorgestuurd naar het PACS. Ook de vorderingen in de tomografische reconstructie werden op de voet gevolgd: de gefilterde terugprojectie werd al gauw vervangen door de iteratieve reconstructie. Het huidige apparatuurspark bestaat uit een eenkopscamera, twee dubbelkopstoestellen en een SPECT/CT. De dienst participeert met twee andere ziekenhuizen in de provincie West-Vlaanderen aan het West-Vlaams PET centrum. Er is echter goede hoop dat met de nakende verandering in de programmering van de PET centra in België een PET toestel kan worden verworven binnen de muren van de dienst; de nodige ruimte werd daarvoor voorzien.

Het personeel van de dienst vóór het secretariaat van de dienst. Van links naar rechts: dr. Anja Van den Eeckhaut, Gino Callant (verantwoordelijk verpleegkundige), dr. Natascha Walgraeve, Stefaan Baert, Sarah Deklerck, Martine Verhelst, Ir. Delphine Vandendriessche (stralingsfysicus), Dorine Danneels, Michel Demeyere. Op de foto ontbreken: Kurt Laforce en dr. Frank De Geeter.

De dienst heeft altijd het voorrecht gehad te beschikken over een geestdriftige en tevreden ploeg van medewerkers. Sommigen onder hen, die nog het begin van de dienst hadden meegemaakt in de kelder van het Oude Sint-Jan zijn al enige tijd op rust, maar hebben een blijvend spoor achtergelaten onder de vorm van technieken die ze mee hebben verfijnd of op punt gesteld, of onder de vorm van een warme benadering van de patiënt, die de dienst nog steeds kenmerkt. Heden ten dage bestaat de ploeg uit vier verpleegkundigen en twee laboratoriumtechnologen. Sinds kort werd de ploeg uitgebreid met een medisch stralingsdeskundige, ingenieur van opleiding, die de dienst mee zal helpen in de ontwikkeling van een kwaliteitssysteem.

Zowat alle courante en enkele minder courante isotopische tests worden uitgevoerd. Tot eind de jaren negentig was er ook een bloeiende afdeling nucleaire geneeskunde in vitro, waar in de hoogdagen een tiental laboratoriumtechnologen waren tewerkgesteld. Bijzonder zijn bijvoorbeeld de overlevingsstudies van bloedplaatjes, die in weinig andere centra gebeuren, maar in ons ziekenhuis met zijn uitgebreide hematologische afdeling een belangrijke plaats hebben verworven. De dienst heeft ook altijd een wetenschappelijke activiteit ontwikkeld en was betrokken bij de vroege multicentrische evaluatie van nieuwe technieken, zoals bijvoorbeeld de FP-CIT scintigrafie bij parkinsonisme, de gated blood pool tomografie, en de behandeling van lymfomen met Zevalin. Met dit profiel schrijft de dienst zich volkomen in het scenario van innovatie dat in de ziekenhuismissie wordt vermeld.

In memoriam Dr. Peter van Urk

Op 2 mei overleed op 72-jarige leeftijd Dr. Peter van Urk, voormalig hoofd Nucleaire Geneeskunde van het St. Antonius Ziekenhuis (te Utrecht, later te Nieuwegein). Velen van ons hebben Peter ooit leren kennen tijdens een van de talrijke advies-, commissie- en bestuursfuncties die hij in diverse gremia binnen de nucleaire geneeskunde heeft bekleed. Steeds gaf hij acte de présence als er weer een beroep op zijn kennis en expertise werd gedaan, ook al interfereerde dat naar zijn zin wel eens te veel met zijn privé leven. Van de vele functies noem ik hier slechts het voorzitterschap van de Nederlandse Vereniging voor Nucleaire Geneeskunde en het hoofdredacteurschap van het Tijdschrift voor Nucleaire Geneeskunde. Hierin bleek bij uitstek hoezeer Peter in staat was het beste in mensen naar boven te halen; zelf trad hij slechts in uitzonderlijke omstandigheden op de voorgrond.
Peter van Urk was een gedreven professional, een zeer toegewijde collega en een bijzonder mens. Wij zullen hem missen.
Mogen zijn nabestaanden de kracht vinden om dit grote verlies te dragen.

Dr. Hans van Isselt

In memoriam Marian Plaizier

Op 23 mei overleed Marian Plaizier, nucleair geneeskundige in het Instituut Verbeeten in Tilburg. Marian begon haar carrière in 1990 in het VUmc. Nadat zij zich enkele jaren had beziggehouden met onderzoek naar beenmergdosimetrie, startte zij in 1992 met de opleiding tot nucleair geneeskundige en werd geregistreerd in 1996. Na de opleiding werkte zij gedurende een jaar in het Catharina Ziekenhuis in Eindhoven. Omdat zich in het Instituut Verbeeten de mogelijkheid van een vaste aanstelling aandiende begon zij daar in 1997. De afdeling nucleaire geneeskunde was toen nog relatief klein en heeft onder haar leiding een groei gekend tot nu vier nucleair geneeskundigen.

Buiten haar dagelijkse werk in de kliniek is Marian een aantal jaren lid geweest van de visitatiecommissie waarbij zij tijdens visitaties de belangen van het vak en de afdelingen nucleaire geneeskunde sterk verdedigde. Zij heeft zich mede beziggehouden met het ontwerpen van een nieuwe vragenlijst in overeenstemming met de NIAZ normen. Korte tijd was zij tweede secretaris van de commissie.
In oktober 2007 werd zij ziek en zij wist toen al dat genezing geen optie was. Ondanks het feit dat zij ziek was en gedurende bijna vijf jaar welhaast maandelijks therapieën moest ondergaan werd er toch nog regelmatig gelachen op de afdeling. Tot begin 2012 heeft zij, de laatste jaren op arbeidstherapeutische basis, gewerkt in het Instituut Verbeeten. Dit was voor haar een welkome afwisseling.

Marian heeft haar privéleven altijd enigszins afgeschermd. Soms vertelde zij en passant over haar zoons die het toch wel goed deden op school. Gezien de intelligentie van Marian was dit waarschijnlijk een understatement. Ook vond zij nog tijd om zich in te zetten voor de Borstkankervereniging Nederland.
Zij wordt door ons herinnerd als de collega die de nucleaire geneeskunde in het Instituut Verbeeten de 21ste eeuw heeft binnengeleid en daarmee veel heeft betekend voor de afdeling.

Rik Pijpers
namens de vakgroep nucleaire geneeskunde Instituut Verbeeten

VANDERWILT

techniques

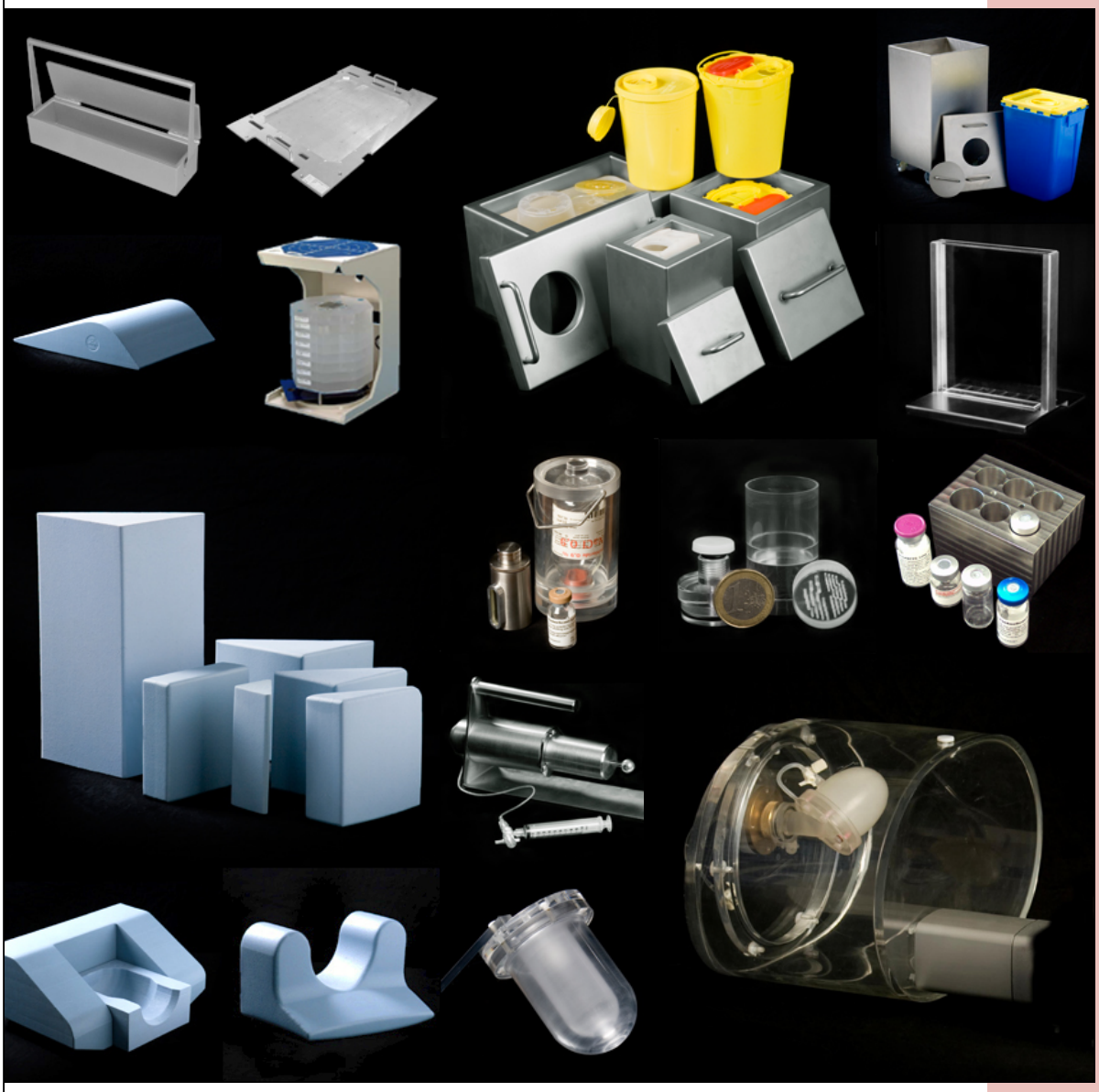

VANDERWILT techniques is a development and manufacturing company, specialised in products for nuclear medicine

T +31 (0)411 68 60 19 | www.for-med.nl

FOR MED

Tijdschrift voor Nucleaire Geneeskunde
ISSN 1381-4842, nr. 2, juni 2013
Uitgever

KLOOSTERHOF
ACQUISITIE SERVICES - UITGEVERIJ

Kloosterhof acquisitie services - uitgeverij
Napoleonsweg 128a
6086 AJ Neer
T 0475 59 71 51
F 0475 59 71 53
E info@kloosterhof.nl
I www.kloosterhof.nl

Hoofdredacteur
prof. dr. J. Booij
j.booij@amc.uva.nl

Redactie
mw. drs. B. Bosveld
mw. drs. F. Celik
dr. J. van Dalen
dr. E.M.W. van de Garde
drs. A.W.J.M. Glaudemans
mw. dr.C.J. Hoekstra
dr. P. Laverman
A. Reniers
dr. H.J. Verberne
dr. O. de Winter

Bureauredactie
Yvonne van Pol-Houben
T 0475 60 09 44
E nucleaire@kloosterhof.nl

Advertentie-exploitatie
Kloosterhof Neer B.V.
acquisitie services – uitgeverij
Eric Vullers
T 0475 597151
E. eric@kloosterhof.nl

Vormgeving
Kloosterhof Vormgeving
Marie-José Verstappen
Sandra Geraedts

Adviesraad
prof.dr. F.J. Beekman
prof.dr. O.C. Boerman
prof.dr. J. Booij
prof.dr. E.F.I. Comans
prof.dr. R.A.J.O. Dierckx
prof.dr. A.A.M.S. van Dongen
prof.dr. B.L.F. van Eck-Smit
prof.dr. P.H. Elsinga
prof.dr.ir. M.de Jong
prof.dr.I. Goethals
prof.dr. O.S. Hoekstra
prof.dr. E.P. Krenning
prof.dr. A.A. Lammertsma
prof.dr. L. Mortelmans
prof.dr. W.J.G. Oyen
prof.dr. A.M.J. Paans
prof.dr. P.P. van Rijk
prof.dr. G.J.J. Teule
dr. R.A. Valdes Olmos

Abonnementen
Leden en donateurs van de aangesloten Leden en donateurs van de aangesloten beroepsverenigingen ontvangen het Tijdschrift voor Nucleaire Geneeskunde kosteloos. Voor anderen geldt een abonnementsprijs van € 45,00 per jaar; studenten betalen € 29,00 per jaar (incl. BTW en verzendkosten).
Voor buitenlandse abonnementen gelden andere tarieven. Opgave en informatie over (buitenlandse) abonnementen en losse nummers (€ 13,50) bij Kloosterhof acquisitie services - uitgeverij, telefoon 0475 59 71 51.
www.tijdschriftvoornucleairegeneeskunde.nl

Verschijningsdata, jaargang 35
Nummer 2: 2 juli 2013
Nummer 3: 1 oktober 2013
Nummer 4: 24 december 2013

Verschijningsdata, jaargang 36
Nummer 1: 1 april 2014
Nummer 2: 1 juli 2014

Aanleveren kopij, jaargang 35
Nummer 3: 1 juli 2013
Nummer 4: 1 oktober 2013

Aanleveren kopij, jaargang 36
Nummer 1: 1 januari 2014
Nummer 2: 1 april 2014

Cursus- en Congresagenda

International Conference on Radiology & Imaging
14 – 16 August, 2013. Chicago-North Shore, USA. www.omicsgroup.com

EANM Course on PET/CT in Oncology, basic
5 – 7 September, 2013. Vienna, Austria. www.eanm.org

Cursus PET farmacokinetiek
11 - 13 september, 2013. Amsterdam, The Netherlands. www.nvng.nl

EANM Cardiovascular Course
14 – 15 September, 2013. Vienna, Austria. www.eanm.org

WMIC 2013
18 – 21 September, 2013. Savannah, USA. www.wmicmeeting.org

BNMS Autumn Meeting
19 September, 2013. Birmingham, UK. www.bnms.org.uk

EANM Technologist PET/CT Course, advanced
21 – 22 September, 2013. Vienna, Austria. www.eanm.org

ASNC 2013
26 – 29 September, 2013. Chicago, USA. www.asnc.org

Lustrumcongres 2013 NVKF
3 – 5 October, 2013. Twente, The Netherlands. www.lustrumnvkf.nl

Jaarlijks congres Nederlandse Vereniging voor Technische Geneeskunde (NVvTG)
11 October, 2013. Utrecht, The Netherlands. www.nvvtg.nl/congres/

EANM '13
19 – 23 October, 2013. Lyon, France. www.eanm.org

Lustrum NVNG
8 November, 2013. Rotterdam, The Netherlands. www.nvng.nl

EANM Dosimetry Course, advanced
14 – 15 November, 2013. Vienna, Austria. www.eanm.org

EANM/ESTRO Educational Seminar on PET in Radiation Oncology
22 – 23 November, 2013. Vienna, Austria. www.eanm.org

EANM Course on PET/CT in Oncology, advanced
28 – 30 November, 2013. Vienna, Austria. www.eanm.org

RSNA 2013
1 – 6 December, 2013. Chicago, USA. www.rsna.org/Annual_Meeting.aspx

2014
3rd Tübingen PET/MR Workshop
17 – 21 February, 2014. Tübingen, Germany. www.pet-mr-tuebingen.de

NuklearMedizin 2014
26 – 29 March, 2014. Hannover, Germany. www.eanm.org

Adreswijzigingen

Regelmatig komt het voor dat wijzigingen in het bezorgadres voor het Tijdschrift voor Nucleaire Geneeskunde op de verkeerde plaats terechtkomen. Adreswijzigingen moeten altijd aan de betreffende verenigingssecretariaten worden doorgegeven. Dus voor de medisch nucleair werkers bij de NVMBR, en voor de leden van de NVNG en het Belgisch Genootschap voor Nucleaire Geneeskunde aan hun respectievelijke secretariaten.
De verenigingssecretariaten zorgen dan voor het doorgeven van de wijzigingen aan de Tijdschrift adresadministratie.
Alleen adreswijzigingen van betaalde abonnementen moeten met ingang van 1 januari 2011 rechtstreeks aan de abonnementenadministratie van Kloosterhof Neer B.V. worden doorgegeven: Kloosterhof Neer B.V., t.a.v. administratie TvNG, Napoleonsweg 128a | 6086 AJ Neer of per E-mail: nucleaire@kloosterhof.nl

Oldelft Benelux Medical Solutions

Mediso AnyScan: de eerste klinische SPECT-CT-PET scanner...

...een unieke oplossing binnen de nucleaire geneeskunde.

Basis configuraties

AnyScan® | AnyScan® SC | AnyScan® PC | AnyScan® S | AnyScan® C

Upgrade door toevoeging

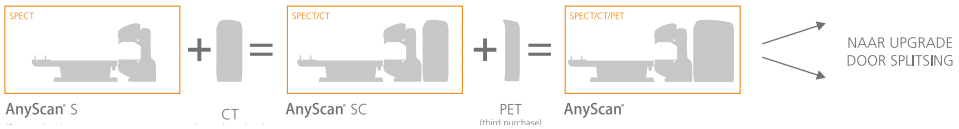

AnyScan® S + CT = AnyScan® SC + PET (third purchase) = AnyScan®

Upgrade door splitsing

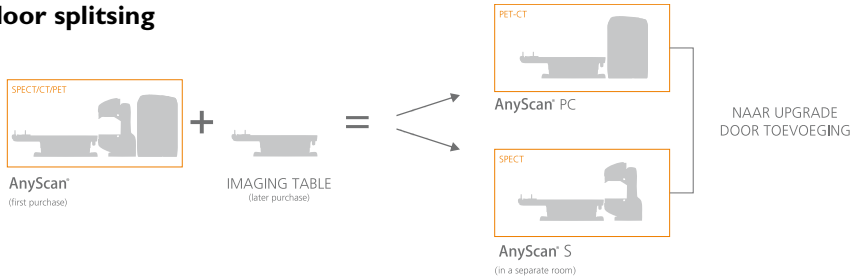

AnyScan® (first purchase) + IMAGING TABLE (later purchase) = AnyScan® PC / AnyScan® S (in a separate room)

Oldelft Benelux heeft reeds meer dan 80 jaar ervaring in de verkoop en service van diagnostische apparatuur en innovatieve healthcare ICT systemen. Zij heeft zich ontwikkeld van producent van apparatuur naar System Integrator en Service Provider voor ziekenhuizen en zorginstellingen.

Met Mediso levert Oldelft Benelux het hele spectrum aan gamma camera's; van kleine enkelkops, tot geavanceerde SPECT-CT-PET combinaties.

Voor meer informatie omtrent de Mediso oplossingen kunt u contact opnemen met uw accountmanager, of stuur een e-mail naar info@oldelftbenelux.nl.

Oldelft Benelux
MEDICAL SOLUTIONS

Oldelft Benelux B.V. Wiltonstraat 41 3905 KW Veenendaal The Netherlands
T +31 318 583 400 F +31 318 583 401 E info@oldelftbenelux.nl I www.oldelftbenelux.nl

GE Healthcare

Improving Heart Failure Risk Assessment

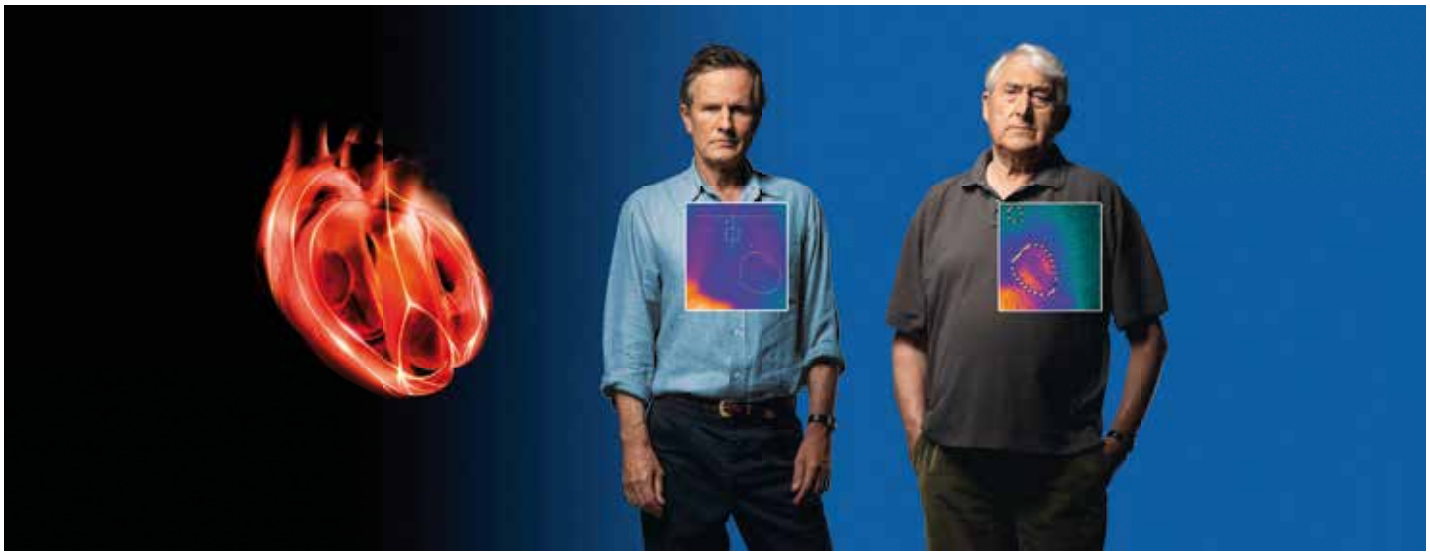

AdreView is a diagnostic agent providing a powerful prognostic insight into heart failure[1]

- Assesses cardiac sympathetic innervation[1]
- Helps predict patients who are at greater or lower risk of heart failure progression, arrhythmias & cardiac death[1]
- Provides a Negative Predictive Value (NPV) of 96% for arrhythmia likelihood & an NPV of 98% for cardiac death likelihood over 2 years[1]
- Provides superior prognostic information in combination with LVEF or BNP compared to LVEF or BNP alone[1]
- Improves heart failure patients' risk assessment and may help clinicians' management decisions[1]

GE imagination at work

AdreView™ Iobenguane I 123 Injection

AdreView is authorised for marketing in the following European countries: Germany, France, Spain, Italy, the United Kingdom, Denmark, Norway, The Netherlands and Belgium.

PRESCRIBING INFORMATION AdreView, Iobenguane (^{123}I) Injection 74 MBq/ml solution for injection
Please refer to full national Summary of Product Characteristics (SPC) before prescribing. Indications and approvals may vary in different countries. Further information available on request.
PRESENTATION Vials containing 74 MBq/ml [^{123}I]Iobenguane at calibration date and hour. Available pack size: 37 to 740 MBq. **DIAGNOSTIC INDICATIONS** • Assessment of sympathetic innervation of the myocardium as a prognostic indicator of risk for progression of symptomatic heart failure, potentially fatal arrhythmic events, or cardiac death in patients with NYHA class II or class III heart failure and LV dysfunction. • Diagnostic scintigraphic localisation of tumours originating in tissue that embryologically stems from the neural crest. These are pheochromocytomas, paragangliomas, chemodectomas and ganglioneuromas. • Detection, staging and follow-up on therapy of neuroblastomas. • Evaluation of the uptake of iobenguane. The sensitivity to diagnostic visualisation is different for the listed pathological entities. The sensitivity is approximately 90% for the detection of pheochromocytoma and neuroblastoma, 70% in case of carcinoid and only 35% in case of medullary thyroid carcinoma (MTC). • Functional studies of the adrenal medulla (hyperplasia). **DOSAGE AND METHOD OF ADMINISTRATION** Cardiology: For adults the recommended dosage is 370MBq. Children under 6 months: 4 MBq per kg body weight (max. 40 MBq), the product must not be given to premature babies or neonates. Children between 6 months and 2 years: 4 MBq per kg body weight (min. 40 MBq). Children over 2 years: a fraction of the adult dosage should be chosen, dependent on body weight (see SPC for scheme). No special dosage scheme required for elderly patients. Oncology: For adults the recommended dosage is 80-200 MBq, higher activities may be justifiable. For children see cardiology. No special dosage scheme required for elderly patients. Administer dose by slow intravenous injection or infusion over several minutes. **CONTRAINDICATIONS** Hypersensitivity to the active substance or to any of the excipients. The product contains benzyl alcohol 10.4 mg/ml and must not be given to premature babies or neonates **WARNINGS AND PRECAUTIONS** Drugs known or expected to reduce the iobenguane(123-I) uptake should be stopped before administration of AdreView (usually 4 biological half-lives). At least 1 hour before the AdreView dose administer a thyroid blockading agent (Potassium Iodide Oral Solution or Lugol's Solution equivalent to 100 mg iodine or potassium perchlorate 400 mg). Ensure emergency cardiac and anti-hypertensive treatments are readily available. In theory, iobenguane uptake in the chromaffin granules may induce a hypertensive crisis due to noradrenaline secretion; the likelihood of such an occurrence is believed to be extremely low. Consider assessing pulse and blood pressure before and shortly after AdreView administration and initiate appropriate anti-hypertensive treatment if needed. This medicinal product contains benzyl alcohol. Benzyl alcohol may cause toxic reactions and anaphylactoid reactions in infants and children up to 3 years old. **INTERACTIONS** Nifedipine (a Ca-channel blocker) is reported to prolong retention of iobenguane. Decreased uptake was observed under therapeutic regimens involving the administration of antihypertensives that deplete norepinephrine stores or reuptake (reserpine, labetalol), calcium-channel blockers (diltiazem, nifedipine, verapamil), tricyclic antidepressives that inhibit norepinephrine transporter function (amitryptiline and derivatives, imipramine and derivatives), sympathomimetic agents (present in nasal decongestants, such as phenylephrine, ephedrine, pseudoephedrine or phenylpropanolamine), cocaine and phenothiazine. These drugs should be stopped before administration of [123I]iobenguane (usually for four biological half-lives to allow complete washout). **PREGNANCY AND LACTATION** Only imperative investigation should be carried out during pregnancy when likely benefit exceeds the risk to mother and foetus. Radionuclide procedures carried out on pregnant women also involve radiation doses to the foetus. Any woman who has missed a period should be assumed to be pregnant until proven otherwise. If uncertain, radiation exposure should be kept to the minimum needed for clinical information. Consider alternative techniques. If administration to a breast feeding woman is necessary, breast-feeding should be interrupted for three days and the expressed feeds discarded. Breast-feeding can be restarted when the level in the milk will not result in a radiation dose to a child greater than 1 mSv. **UNDESIRABLE EFFECTS** In rare cases the following undesirable effects have occurred: blushes, urticaria, nausea, cold chills and other symptoms of anaphylactoid reactions. When the drug is administered too fast palpitations, dyspnoea, heat sensations, transient hypertension and abdominal cramps may occur during or immediately after administration. Within one hour these symptoms disappear. Exposure to ionising radiation is linked with cancer induction and a potential for development of hereditary defects. For diagnostic nuclear medicine investigations the current evidence suggests that these adverse effects will occur with low frequency because of the low radiation doses incurred. **DOSIMETRY** The effective dose equivalent resulting from an administered activity amount of 200 MBq is 2.6 mSv in adults. The effective dose equivalent resulting from an administered activity amount of 370 MBq is 4.8 mSv in adults. **OVERDOSE** The effect of an overdose of iobenguane is due to the release of adrenaline. This effect is of short duration and requires supportive measures aimed at lowering the blood pressure. Prompt injection of phentolamine followed by propanolol is needed. Maintain a high urine flow to reduce the influence of radiation. **CLASSIFICATION FOR SUPPLY** Subject to medical prescription (POM).**MARKETING AUTHORISATION HOLDERS.** DE: GE Healthcare Buchler GmbH & Co. KG, 18974.00.00. DK: GE Healtcare B.V., DK R. 1013. FR: GE Healthcare SA, NL 18599. NL: GE Healthcare B.V., RVG 57689. NO: GE Healthcare B.V., MTnr. 94-191. **DATE OF REVISION OF TEXT** 9 August 2010 .

GE Healthcare Limited, Amersham Place, Little Chalfont, Buckinghamshire, England HP7 9NA
www.gehealthcare.com

References: 1. Jacobson AF *et al.* Myocardial Iodine-123 *Meta*-Iodobenzylguanidine Imaging and Cardiac Events in Heart Failure. Results of the Prospective ADMIRE-HF (AdreView Myocardial Imaging for Risk Evaluation in Heart Failure) Study. J Am Coll Cardiol 2010;55.

10-2010 JB4260/OS INT'L ENGLISH